molecular pharmaceutics

pubs.acs.org/molecularpharmaceutics

Article

Effect of Extracellular Matrix Coating on Cancer Cell Membrane-Encapsulated Polyethyleneimine/DNA Complexes for Efficient and Targeted DNA Delivery In Vitro

Liang Liu,* Yiran Chen, Chaobing Liu, Yujian Yan, Zhaojun Yang, Xin Chen, and Gang Liu

Cite This: *Mol. Pharmaceutics* 2021, 18, 2803−2822

Read Online

ACCESS | Metrics & More | Article Recommendations

ABSTRACT: Polyethyleneimine (PEI) has a good spongy proton effect and is an excellent nonviral gene vector, but its high charge density leads to the instability and toxicity of PEI/DNA complexes. Cell membrane (CM) capsules provide a universal and natural solution for this problem. Here, CM-coated PEI/DNA capsules (CPDcs) were prepared through extrusion, and the extracellular matrix was coated on CPDcs (ECM-CPDcs) for improved targeting. The results showed that compared with PEI/DNA complexes, CPDcs had core−shell structures (PEI/DNA complexes were coated by a 6−10 nm layer), lower cytotoxicity, and obvious homologous targeting. The internalization and transfection efficiency of 293T-CM-coated PEI70k/DNA capsules (293T-CP70Dcs) were 91.8 and 74.5%, respectively, which were higher than those of PEI70k/DNA complexes. Then, the internalization and transfection efficiency of 293T-CP70Dcs were further improved by ECM coating, which were 94.7 and 78.9%, respectively. Then, the internalization and transfection efficiency of 293T-CP70Dcs were further improved by ECM coating, which were 94.7 and 78.9%, respectively. Moreover, the homologous targeting of various CPDcs was improved by ECM coating, and other CPDcs also showed similar effects as 293T-CP70Dcs after ECM coating. These findings suggest that tumor-targeted CPDcs may have considerable advantages in gene delivery.

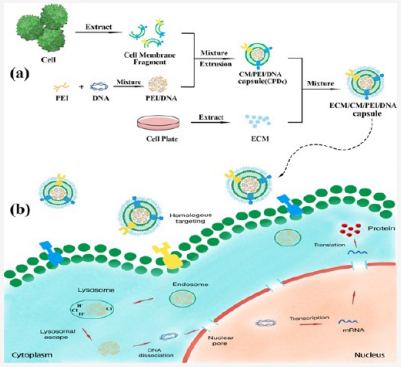

KEYWORDS: *cell membrane-encapsulated, DNA delivery, polyethyleneimine, homologous targeting*

1. INTRODUCTION

Gene therapy shows the potential to treat a wide range of different diseases caused by defective gene expression levels, such as many types of cancer.[1,2] Its most common implement method is to deliver therapeutic genetic materials into cells to re-establish protein levels by restoring or altering the gene expression.[3,4] However, the efficient delivery of nucleic acid-based biomolecules remains prohibitively challenging and requires controllable[5] and nontoxic[6] delivery vectors. In addition to gene transfer efficiency, the delivery to tumor cells must exhibit tissue specificity.[7] Nucleic acids are delivered to cells via different nonviral vectors, such as lipoplexes and polyplexes.[8] Although these materials are effective delivery agents in in vitro experiments, they are often ineffective when used in vivo. Even if their ability to deliver genes is maintained, additional modifications are needed to achieve tissue specificity.[9,10]

Among various cationic polymers, PEI has been widely used as a benchmark polymeric vector.[11,12] PEI condenses DNA to nanosized complexes (polyplexes) to facilitate endocytosis. Once inside the cell, the PEI exhibits its proton sponge effect, buffering, and membrane lytic capacity to benefit the endosomal escape of polyplexes.[13] However, its inherent cytotoxicity caused by its highly positive charge and lack of gene transfer targeting ability limits its clinical application.[14] One strategy to improve PEI is to graft it with central or negatively charged molecules; for example, polysaccharides and PEG have been used to modify PEI to obtain gene carriers with low toxicity and high efficiency due to their good biological compatibility.[15−17] However, the amino content in the PEI molecule is decreased due to grafting, thus weakening its DNA condensation ability.[18] In addition, the stability and transfection efficiency of the vector/gene complex formed by grafting PEI and DNA are not substantially improved compared with those of PEI/DNA.[19,20] To solve this problem, researchers proposed another strategy of using nonionic hydrophilic PEG, negatively charged liposomes, degradable polymers,[21] polysaccharide-based polyanions (alginate[22] and hyaluronic acid[23]), and proteins (transferrin[24]) to covalently couple with or be coated on the PEI/DNA complexes. The

Received: April 29, 2021
Revised: May 26, 2021
Accepted: May 27, 2021
Published: June 4, 2021

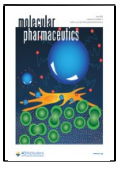

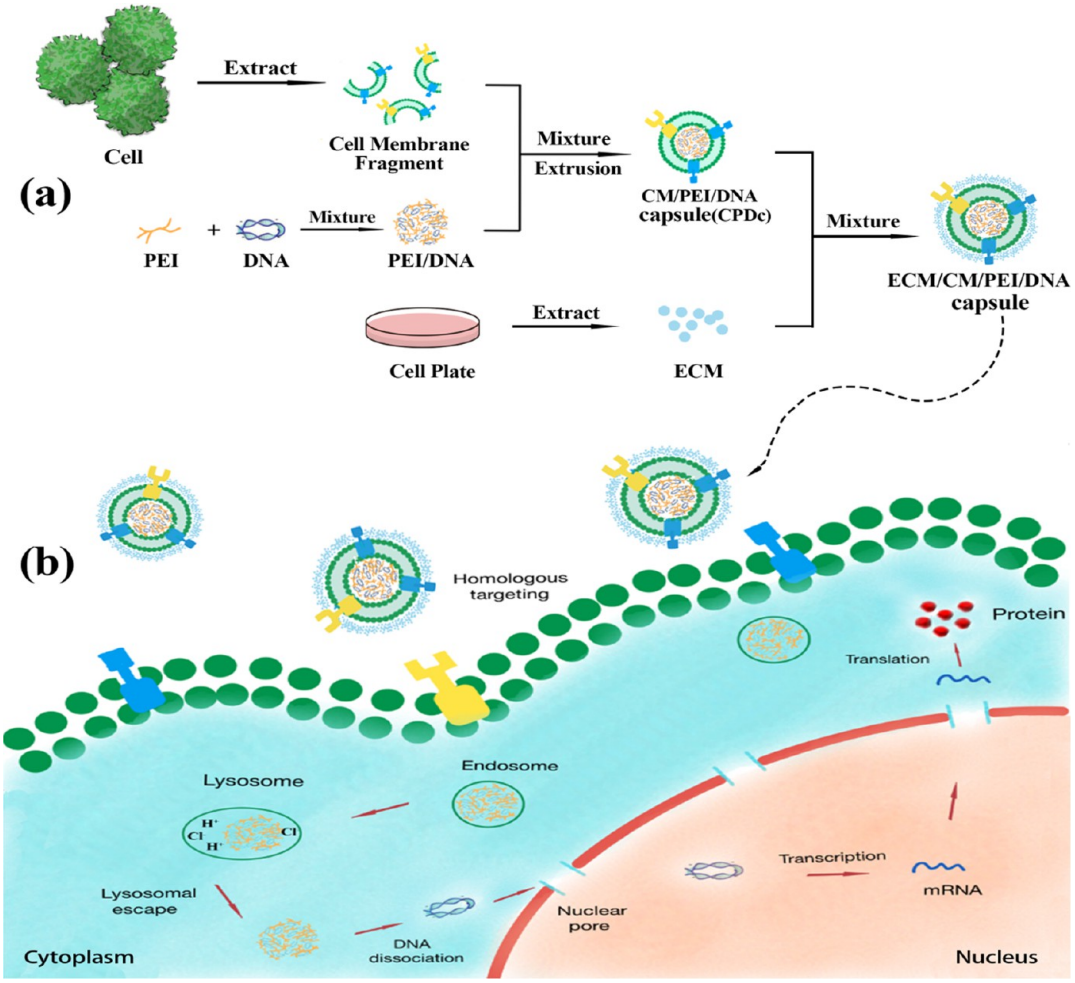

Figure 1. Schematic illustration of the in-cell transportation process of CPDc. (a) Preparation scheme of various CPDcs. (b) Transport and gene transfection of CPDc in the cell.

modifications shielded against the positive charge, reduced toxicity, prevented aggregation caused by salt and serum albumin, and even achieved tumor targeting.[25]

Phospholipid is one of the main components of the cell membrane, which has high biocompatibility and has been applied for drug delivery in clinics.[26] In recent years, liposomes with phospholipid as the main component have been used to wrap PEI/DNA complexes to form capsules. Compared with the unmodified complexes, these capsules have the advantages of reducing the surface charge significantly, higher transfection efficiency, lower cytotoxic, and high stability. In addition, in vivo studies also show that liposome embedding can prolong the blood circulation time of the PEI/DNA complex without significant toxicity. Therefore, liposome embedding is considered to be a potential strategy for gene vector construction.[27−29] Cell membrane (CM) coating has become an effective biomimetic method to camouflage nanoparticles for optimized cancer treatment.[30] The cell membranes have properties and structures similar to liposomes. In addition, the adhesion protein, antigen, and membrane structure of the source CM can be retained on the surface of the nanoparticles coated with the CM.[31] Therefore, membrane camouflage nanoparticles can exhibit the related surface properties and functions of natural CMs. For example, the red blood CM has the inherent ability of immune escape, prolongs blood circulation time, and has been used to camouflage perfluorocarbon, polymer, silica, and magnetic/metal−organic framework nanoparticles for imaging-guided cancer radiotherapy and chemotherapy.[32−35] The cancer CM undergoes homologous binding, and it can enhance the targeted delivery of drug nanoparticles in tumors.[36] Other homing cell lines, such as platelets, have been applied to encapsulate iron oxide nanoparticles for magnetic resonance imaging-guided cancer phototherapy.[37] However, the bionic method is rarely used to enhance the delivery efficiency of gene delivery materials, especially PEI-based gene carriers.

The extracellular matrix (ECM), which is distributed outside the cell, is a network structure composed of proteins and polysaccharides secreted by cells. Its components in animal cells have three types and functions: (1) structural proteins, including collagen and elastin, which impart strength and toughness to the ECM; (2) proteoglycans that are covalently formed by proteins and polysaccharides, have high hydrophilicity, and impart stress resistance to the ECM; and (3) adhesion glycoproteins, including fibronectin and laminin, which improve cell adherence to the ECM.[38−40]

Inspired by the new CM coating strategy, this study developed three kinds of cancer CM-modified PEI/DNA capsules (CPDcs) to reduce the toxicity and strengthen the targeting of PEI/DNA complexes as a DNA delivery platform. As shown in Figure 1, CPDcs were prepared following a basic method and then characterized by various techniques, such as

https://doi.org/10.1021/acs.molpharmaceut.1c00359
Mol. Pharmaceutics 2021, 18, 2803−2822

dynamic light scattering (DLS), ζ-potential, transmission electron microscopy (TEM), and sodium dodecyl sulfate-polyacrylamide gel electrophoresis (SDS-PAGE). The potential of CPDc as a gene vector was systematically studied by examining its DNA carrying capacity, protection ability, release ability, cell uptake efficiency, transfection efficiency, and safety. Finally, the influence of the ECM on CPDc targeting was evaluated. This work tries to provide a new strategy for the design and development of PEI-based gene vectors.

2. MATERIALS AND METHODS

2.1. Materials. Branched polyethylenimine (bPEI, M_w = 30, 70 kDa) was purchased from Macklin Biochemical Co., Ltd. (Shanghai, China). Fluorescein isothiocyanate (FITC), fluorescent dyes of ethidium bromide (EtBr), and DiI (CM red fluorescent probe) were obtained from Sigma-Aldrich, Inc. (Shanghai, China). The EGFP plasmid was amplified in *Escherichia coli* and isolated using a Maxi plasmid kit purchased from Tiangen Biotechnology Co., Ltd. (Beijing, China). 3-[4,5-Dimethylthiazol-2-yl]-2,5-diphenyltetrazolium bromide (MTT) and dimethyl sulfoxide (DMSO) were bought from Sinopharm Co., Ltd. (Shanghai, China). Fetal bovine serum (FBS), Dulbecco's modified Eagle's medium (DMEM), and Active Ingredient−Active Ingredient solution (100×) were acquired from Gibco (Shanghai, China). 293T, HeLa, and HepG2 cells were purchased from the National Center Cell Bank Introduction (Beijing, China) and cultured in the DMEM medium with 10% FBS and 1% Active Ingredient−Active Ingredient at 37 °C in a 5%CO_2 atmosphere.

2.2. Preparation of CM. The adherent 293T, HeLa, and HepG2 cells were digested with trypsin and centrifuged at 3000 rpm at 4 °C for 3 min, and the culture medium was discarded. The cells were resuspended with 4 °C prefrozen isotonic 1× PBS buffer and centrifuged at 4 °C at 3000 rpm for 3 min, and the supernatant was removed. After washing three times, the cells were added with PBS buffer solution, frozen at 4 °C for 30 min, swelled in the hypotonic solution, and frozen in liquid nitrogen for 8 s. The cells were removed and restored to liquid at room temperature (RT) and then frozen in liquid nitrogen. After repeated freezing and thawing five times, centrifugation was performed at 4 °C at 14 800 rpm for 10 min. The supernatant was discarded, and the precipitate was resuspended with sterile water before freeze-drying. The obtained solid CM fragments were resuspended in sterile water to prepare 1 mg/mL suspension and stored at −20 °C.

2.3. Preparation of CPDcs. CPDcs were prepared through extrusion. PEI30k and DNA were mixed at an optimum mass ratio of 2.5/1, which was calculated by evaluating the transfection efficiency at different mass ratios of PEI to DNA. The mixture was incubated at RT for 30 min to prepare the PEI/DNA complex. The CM suspension was thawed at RT, mixed with the PEI30k/DNA complex at the mass ratios of 0.5/2.5/1, 1/2.5/1, 2/2.5/1, 3/2.5/1, and 4/2.5/1, and incubated at RT for 30 min after vortexing for 1 min. The mixture of CM and PEI/DNA was extruded through a polycarbonate membrane with an aperture of 200 nm by a mini extruder (Morgec, Shanghai, China). After repeated extrusion 15 times, the mixture was centrifuged at 14 800 rpm for 10 min. The supernatant was collected and precipitated to obtain the CM/PEI30k/DNA capsule (CP30Dc). The prepared CPDcs were dispersed in sterile water at a concentration of 1 mg/mL and stored at −20 °C. Additional CPDcs with PEI70k (CP70Dc) and other CMs were prepared by the same method. The mass ratios of CP70Dc were 0.5/0.75/1, 1/0.75/1, 2/0.75/1, 3/0.75/1, and 4/0.75/1. The various CPDcs prepared using 293T, HepG2, and HeLa-CM were named as 293T-CPDc, HepG2-CPDc, and HeLa-CPDc, respectively. The various CPDcs were prepared with PEI30k and PEI70k, and different CMs were labeled as 293T-CP30Dc, HepG2-CP30Dc, HeLa-CP30Dc, 293T-CP70Dc, HepG2-CP70Dc, and HeLa-CP70Dc.

2.4. Preparation of ECM. 293T cells were seeded in six-well plates at a density of 2.5×10^5 per well and cultured at 37 °C in a 5% CO_2 atmosphere. After 24 h, the plates containing the complete medium were frozen at −80 °C for 12 h. At room temperature, the medium was thawed and removed, and then the plate was washed three times with HbSS buffer to remove the cell debris. The ECM can be obtained on the surface of the plate after vacuum freeze-drying, and the yield of the ECM can be calculated by weighing the mass change of the plate before and after the experiment. Finally, the ECM was dissolved in sterile deionized water, and the storage solution with a concentration of 1 mg/mL was prepared and stored at −20 °C for future use. The ECM of HeLa and HepG2 cells were prepared by the same method.

2.5. Preparation of ECM-CPDc. First, 293T-CP70Dc, HepG2-CP70Dc, and Hela-CP70Dc with a mass ratio of 2/0.75/1 were prepared according to the method in Section 2.3. Then, the extracellular matrix (ECM) of 293T, HepG2, and HeLa cells were, respectively, added into the corresponding CP70Dcs for vortex mixing, and the final mass ratio was controlled to be 2/2/0.75/1. ECM-293T-CP70Dc, ECM-HepG2-CP70Dc, and ECM-Hela-CP70Dc were prepared by extrusion with the Genizer liposome extruder.

2.6. SDS-PAGE. SDS-PAGE analysis was conducted to verify the preparation of CPDcs and the retention of CM surface proteins. CPDcs, 293T-CM suspensions, and PEI/DNA complexes were diluted to 1 mg/mL, then mixed with the loading buffer, and incubated in boiling water for 5 min. Then, the mixtures were loaded into the concentration gel, and electrophoresis was performed at 150 V for 20 min and then continued for 1 h at 200 V. Three percent of concentration gel and 10% of separation gel were chosen as electrophoresis plastic, low-molecular-weight standard protein as a marker for electrophoresis. After electrophoresis, the gel was dyed with a simple blue working fluid for 2 h, then decolorized with a decolorizing liquid, and observed and imaged by a gel imaging system (Gel Doc XR, Bio-Rad).

2.7. DLS and ζ-Potential. Particle size and ζ-potential directly affect the cell uptake efficiency and transfection efficiency of the vector/gene polyplexes. The particle size of 293T-CPDc with different mass ratios was analyzed by dynamic light scattering (DLS). 293T-CP30Dcs with different mass ratios (0.5/2.5/1, 1/2.5/1, 2/2.5/1, 3/2.5/1, and 4/2.5/1) were prepared according to Section 2.3 and diluted to 4 mL with deionized water. The average particle size and ζ-potential of 293T-CP30Dcs were obtained from the average values of the three determinations with a standard deviation of ±SD as measured by a Zetasizer Nano ZS (Malvern, U.K.) at 25 °C. The same method was applied for various CP70Dcs and ECM-CP70Dcs.

2.8. TEM. CPDc morphology was observed using a TEM. The prepared 293T-CP70Dcs (Section 2.3) were deionized and dispersed to an appropriate concentration (DNA concentration was 0.05 mg/mL), and then 50 μL of CP70Dc dispersion was dripped onto the copper mesh. After

https://doi.org/10.1021/acs.molpharmaceut.1c00359
Mol. Pharmaceutics 2021, 18, 2803−2822

drying at RT, the morphology of the samples was observed using a TEM (JEM-F200, JEOL, Japan).

2.9. Agarose Gel Electrophoresis. Agarose gel electrophoresis was used to screen and determine the optimum mass ratio to prepare the PEI/DNA complex and evaluate the DNA protection and releasing ability of CPDc. PEI and DNA with different mass ratios were mixed at RT for 30 min to determine the optimum mass ratio of the PEI/DNA complex. The mixtures were loaded to 1% agarose gel containing ethidium bromide, and electrophoresis was performed at 90 V for 40 min. Finally, a gel imaging system (Gel Doc XR, Bio-Rad) was used to image the gel. In this experiment, the mass ratios of PEI30k/DNA were 0, 0.125/1, 0.25/1, 0.5/1, 1/1, 1.5/1, 2/1, 2.5/1, and 3/1, and those of PEI70k/DNA were 0, 0.125/1, 0.25/1, 0.5/1, 0.75/1, 1/1, 1.5/1, 2/1, and 2.5/1. For DNA protection and release evaluation, PEI70k/DNA with a mass ratio of 0.75/1 and 293T-CP70Dc with a mass ratio of 2/0.75/1 were prepared (Section 2.3). The amount of DNA in each sample was 0.4 μg. Five sample groups were set up. The first group was composed of DNA, PEI70k/DNA complexes, and 293T-CP70Dc. The second group was prepared by adding deionized water, DNase I, and PBS buffer (pH 7.4) to the three samples of the first group and incubated at 37 °C for 2 h. The third group was synthesized by adding 4 μL of Active Ingredient sodium (20 mg/mL) to the first group and incubating the mixture at 37 °C for 2 h. For the fourth group, deionized water, nuclease DNase I, and PBS buffer (pH 7.4) were added to the first group samples, incubated for 2 h at 37 °C, then added with 4 μL of Active Ingredient sodium (20 mg/mL), and incubated at 37 °C for 2 h. For the fifth group, DNA, PEI70k/DNA complex, and 293T-CP70Dc were individually added with 4 μL of Active Ingredient sodium (20 mg/mL), incubated at 37 °C for 2 h, added with deionized water, nuclease DNase I, and PBS buffer (pH 7.4), respectively, and then incubated at 37 °C for 2 h. Finally, all groups were loaded to 1% agarose gel containing ethidium bromide, and electrophoresis was performed at 90 V for 40 min. The mass ratios of PEI70k/DNA and 293t-CP70Dc were 0.75/1 and 2/0.75/1, respectively.

2.10. Determination of Encapsulation Efficiency (EE). The PEI/DNA complex with a mass ratio of 2.5/1 was prepared with DAPI-labeled DNA. The fluorescence intensity ($FI_{PEI/DNA}$) of the system at 454 nm (λ_{ex} = 364 nm) was measured using a microplate reader (Enspire, PerkinElmer). CPDcs were prepared through extrusion (Section 2.3) 10, 15, and 20 times. The mass ratios of 293T-CP30Dc were 0.5/2.5/ 1, 1/2.5/1, 2/2.5/1, 3/2.5/1, and 4/2.5/1, and those of 293T-CP70Dc were 0.5/0.75/1, 1/0.75/1, 2/0.75/1, 3/0.75/1, and 4/0.75/1. After the centrifugation of the CDPc suspension at 14 800 rpm for 10 min, the fluorescence intensity of the supernatant at 454 nm ($FI_{supernatant}$) was determined. The EE of the CM for PEI/DNA was calculated using formula 1. In this assay, three repeats were set for each sample, and the average value was calculated from three measurements. The standard deviation was ±SD. $EE(\%) = [FI_{PEI/DNA} - FI_{supernatant}/FI_{PEI/DNA}] \times 100\%$, formula 1.

2.11. MTT Assay. Biocompatibility is an important index to evaluate the performance of gene vectors. The effects of different CPDcs on the viability of 293T, HeLa, and HepG2 cells were studied by the MTT assay to evaluate the biological safety of these capsules. All kinds of CPDcs were prepared (Section 2.3), and their mass ratio was consistent with that in Section 2.7. When their density reached 80−90%, the cells were digested with trypsin and suspended into a single cell suspension in DMEM. Then, the cells were seeded into a 96-well plate and cultured in a 5% CO_2 atmosphere at 37 °C. After 24 h, the cells were cultured with 100 μL of DMEM dispersion containing different mass ratio samples instead of the original medium for 24 h. The culture medium was then removed, the cells were washed with Hanks buffer three times, and 100 μL of MTT solution (5 mg/mL) was added. After 4 h of culture, the MTT was removed, and 100 μL of DMSO was added to completely dissolve the purple crystal metabolites. Absorbance at 570 nm (A_{570}) was measured with a microplate reader (Enspire, PerkinElmer). The cell survival rate was calculated according to formula 2. The mean cell survival rate was calculated from the results of each three replicates, and the standard deviation was ±SD (n = 3). The cell survival rate = (A1/A0) × 100% (formula 2), where A0 is the absorbance measured at 570 nm of the sample treated with complete medium, and A1 is the absorbance measured at 570 nm of the sample treated with different CPDcs.

2.12. Cell Uptake Efficiency of CPDc. CPDcs were prepared with FITC-labeled PEI to study their cellular uptake conveniently. In brief, 9 mg of FITC was dissolved in 2.5 mL of dimethyl sulfoxide (DMSO), mixed with 7.5 mL of an aqueous solution containing 100 mg of PEI30k, and stirred at RT in the dark for 24 h. The mixture was dialyzed in a dialysis bag with a molecular weight cut-off of 1000 Da to remove free FITC. The retention fluid was freeze-dried to obtain FITC-labeled PEI30k (FITC-PEI30k). FITC-labeled PEI70k (FITC-PEI70k) was prepared using the same method. CPDcs with FITC-labeled PEI were prepared according to Section 2.3. The cells were cultured in a DMEM medium containing 10% FBS at 37 °C in a 5% CO_2 atmosphere. When their growth density reached 80−90%, the cells were seeded onto a 12-well plate with cell climbing plates at a density of 1×10^5 cells/well and cultured at 37 °C in a 5% CO_2 atmosphere for 24 h. DMEM containing various 293T-CP30Dcs was used to replace the original culture medium. After 4 h, the DMEM was removed, and the cells were washed with HbSS buffer three times. Each well was added with 1 mL of 4% paraformaldehyde solution, and the cells were fixed at RT for 15 min. After paraformaldehyde was removed, the cells were washed with HbSS buffer three times and then stained with DAPI for 30 min. Finally, the cell uptake of different complexes was observed using a confocal laser microscope (Stellaris 6, Leica, GER). Flow cytometry was used to quantitatively measure the cell uptake efficiency. After coculturing with different 293T-CP30Dc for 4 h, the cells were digested with trypsin and dispersed in DMEM, and their uptake efficiency was detected by flow cytometry (DxFLEX, Beckman). Three parallel samples were set for each sample, and the average cell uptake efficiency was calculated from three measurements with a standard deviation of ±SD. The cellular uptake of FITC-PEI30k/DNA and FITC-PEI70k/DNA complexes was used as the control. The amount of DNA in each well was 2 μg. CPDcs were prepared and doped with the ECM to study the effect of the latter on the targeting of the former. Uptake efficiency in different cells was studied using the same method. FITC-labeled PEI70k was selected to prepare 293T-CP70Dc, and ECM-CP70Dcs were prepared through extrusion according to Section 2.5.

2.13. Cell Uptake Mechanism of CPDc. PEI/DNA complexes and different CP70Dcs were prepared according to the scheme in Section 2.3. The prepared complex was

https://doi.org/10.1021/acs.molpharmaceut.1c00359
Mol. Pharmaceutics 2021, 18, 2803−2822

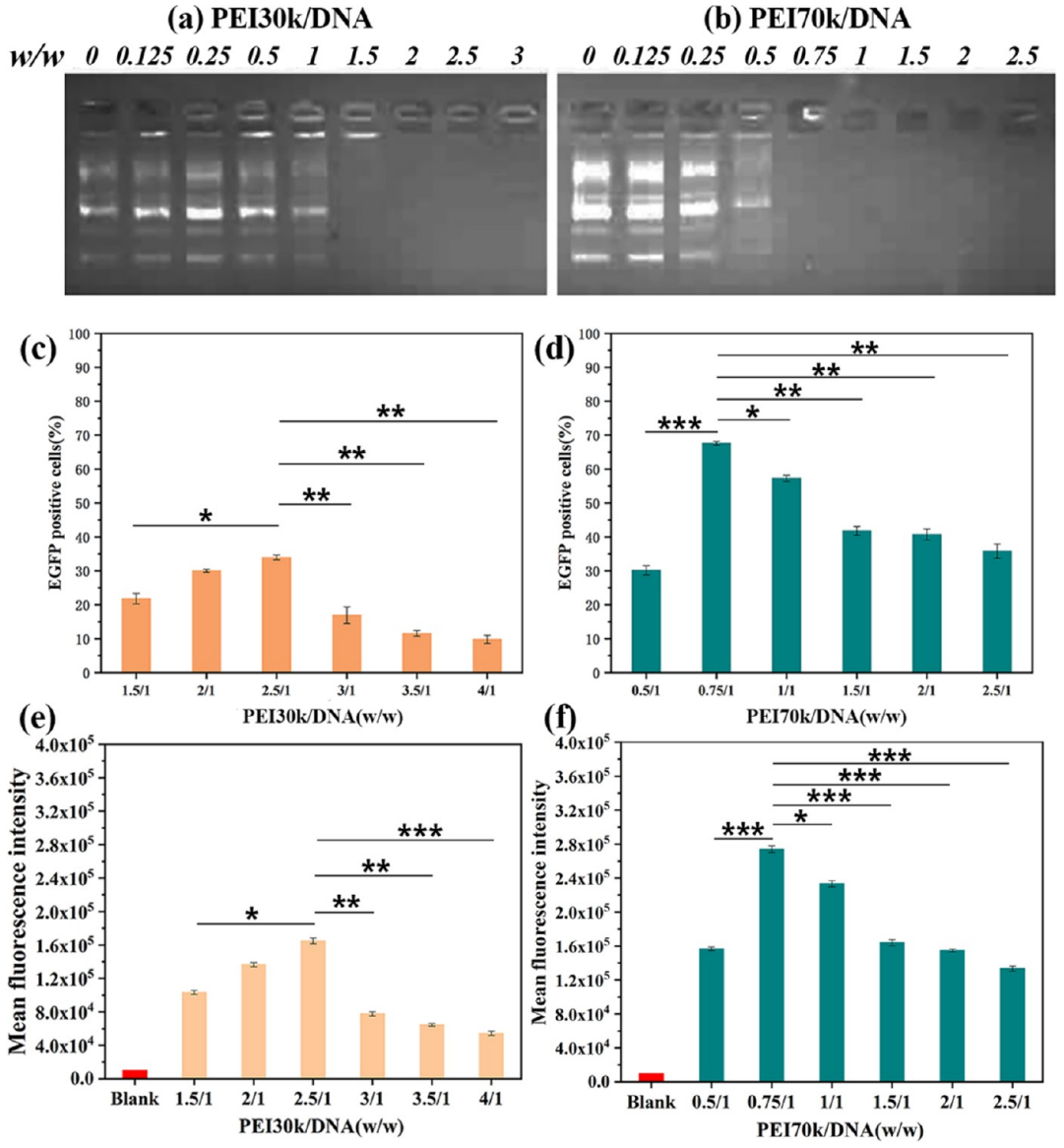

Figure 2. Selection of the optimum mass ratio for PEI/DNA preparation. (a) Agarose gel electrophoresis results of PEI30k/DNA. (b) Agarose gel electrophoresis results of PEI70k/DNA. (c) EGFP expression efficiency of PEI30k/DNA complexes in 293T cells measured by flow cytometry. (d) EGFP expression efficiency of PEI70k/DNA complexes in 293T cells measured by flow cytometry. (e) Mean fluorescence intensity of GFP positive expression cells treated with PEI30k/DNA. (f) Mean fluorescence intensity of GFP positive expression cells treated with PEI70k/DNA. (mean ± SD, $n = 3$, $^{*}p \leq 0.05$, $^{**}p \leq 0.01$, $^{***}p \leq 0.0005$).

dispersed in 200 μL of DMEM. 293T cells were seeded in 24-well plates (1×10^5 cells per well) and cultured at 37 °C in a 5% CO_2 atmosphere for 24 h. When the confluence reached 80%, the cells were washed once with 1× PBS and cultured in a complete medium containing transport inhibitor: Active Ingredient (final concentration of 0.03 mmol/L), or methyl β-cyclodextrin (final concentration of 10 mmol/L), or Active Ingredient (final concentration of 2.5 mmol/L) for 1 h. After that, the DMEM dispersion was used to replace the medium in each well. After 4 h, the medium was removed and the cells were washed twice with PBS. Flow cytometry was used to measure the cell uptake efficiency, and the average value was taken three times in each group. Finally, Flowjo 10.4 software was used to process the data. DMEM-treated cells were set as a control group.

2.14. In Vitro Gene Transfection. The cells were seeded in 24-well plates at a density of 5×10^4 cells/well, and then cultured in a complete medium containing 10% FBS at 37 °C in a 5% CO_2 atmosphere for 24 h until their density reached 70−80%. DMEM was used to replace the complete medium, and the cells were cultured for 2 h. After the cells were cocultured with DMEM dispersions of 293T-CP30Dc for 4 h, the DMEM dispersions of samples were replaced with a complete medium. The cells were cultured for 44 h and then fixed with paraformaldehyde (Section 2.10). EGFP-positive cells were observed using a fluorescence microscope. Quantitative transfection efficiency was measured by flow cytometry. Three parallel samples were set for each specimen, and the average cell uptake efficiency was calculated from three measurements with a standard deviation of ±SD. 293T-CP30Dcs were prepared and doped with the ECM to study the effect of the latter on the transfection efficiency of the former. The same method was used to determine the transfection

https://doi.org/10.1021/acs.molpharmaceut.1c00359
Mol. Pharmaceutics 2021, 18, 2803−2822

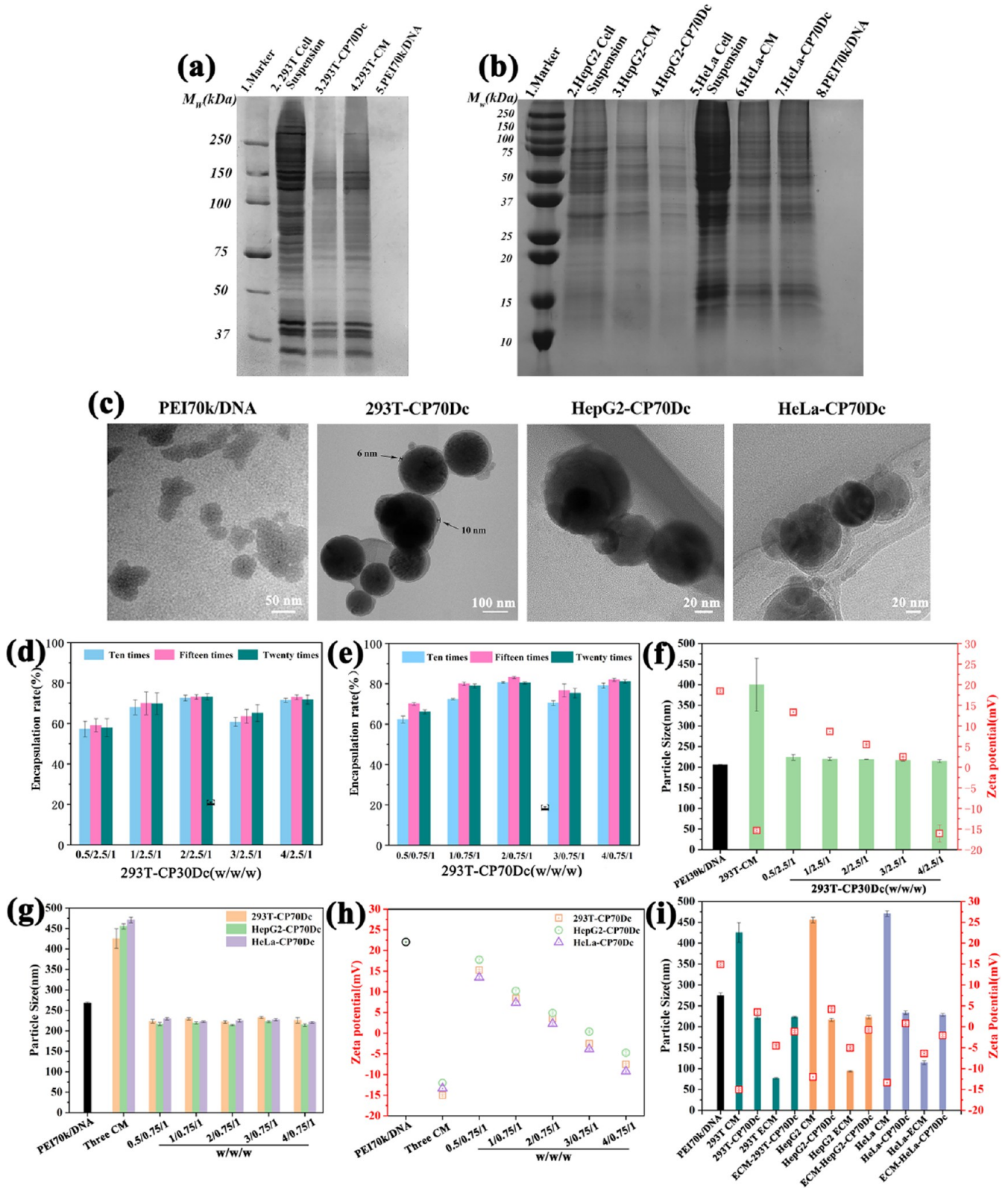

Figure 3. Characterization results of CPDc. (a) SDS-PAGE electrophoresis analysis results of 293T-CP70Dc. (b) SDS-PAGE electrophoresis analysis results of HepG2-CP70Dc and HeLa-CP70Dc. (c) TEM images of PEI70k/DNA and various CP70Dcs. (d) Encapsulation efficiency of 293T-CP30Dc. (e) Encapsulation efficiency of 293T-CP70Dc. (f) Particle size and ζ-potential of 293T-CP30Dc. (g) Particle size and ζ-potential of 293T-CP70Dc, HepG2-CP70Dc, and HeLa-CP70Dc. (h) ζ-Potential of 3T-CP70Dc, HepG2-CP70Dc, and HeLa-CP70Dc. (i) Comparison of particle size and ζ-potential of PEI70k/DNA complexes, various CMs, ECMs, CP70Dcs, and ECM-CP70Dcs. All ECM-CP70Dcs were prepared at a mass ratio of 1/2/0.75/1 by the liposome extrusion method (mean ± SD, n = 3).

https://doi.org/10.1021/acs.molpharmaceut.1c00359
Mol. Pharmaceutics 2021, 18, 2803−2822

efficiency in different cells and in 293T-CP70Dc and ECM-293T-CP70Dc.

2.15. Statistics and Software. Statistical analyses were performed using GraphPad Prism software. Data analyses were performed with Student's *t*-test and one-way analysis of variance (ANOVA). $p < 0.05$ was considered to be statistically significant.

3. RESULTS AND DISCUSSION

3.1. Preparation and Characterization of CPDc.

3.1.1. Determination of Mass Ratio of PEI/DNA. For the successful preparation of CPDc as a safe and efficient gene carrier, the DNA condensation ability of different molecular weight PEI (PEI30k, PEI70k) was investigated at different mass ratios to determine the optimum mass ratio of PEI/DNA that can condense DNA completely. Furthermore, the transfection efficiency of the PEI/DNA complex at different mass ratios was examined to determine the optimal PEI/DNA mass ratio and PEI molecular weight for the preparation of CPDcs. The DNA condensation ability of PEI is verified by the gel retardation assay. Figure 2a,b shows that DNA was completely condensed by PEI30k and PEI70k at the mass ratios of 2/1 and 0.75/1, respectively. PEI70k showed stronger DNA condensation ability than PEI30k, which was consistent with the previous reports.[38] However, the cytotoxicity caused by the high molecular weight of PEI70k might also affect the transfection efficiency of the PEI/DNA complex.[38] Therefore, the gene transfection efficiency of the PEI/DNA complex at different mass ratios was studied to further determine the optimal PEI/DNA mass ratio for CPDc preparation. Figure 2c,d shows that the highest transfection efficiencies of 38.6% and 68.2% were achieved by PEI30k/DNA and PEI70k/DNA70k, respectively, at the mass ratios of 2.5/1 and 0.75/1, respectively. PEI70k/DNA showed higher transfection efficiency than PEI30k/DNA in various mass ratios. On this basis, the best quality ratio of PEI/DNA for CPDc preparation was 2.5/1 (PEI30k/DNA) and 0.75/1 (PEI70k/DNA). Owing to its relatively high transfection efficiency, PEI70k/DNA might be suitable for the preparation of CPDc as an efficient DNA delivery vector. Therefore, to obtain the most effective gene delivery system, PEI70k was selected to prepare CPDc and used in subsequent research, and the optimal mass ratio was 0.75/1. As shown in Figure 2e,f, the mean fluorescence intensity of GFP positive cells showed the same trend as that of flow cytometry analysis. PEI30k/DNA and PEI70k/DNA complexes showed the best transfection efficiency at 2.5/1 and 0.75/1, respectively. Therefore, these mass ratios of PEI/DNA complexes with the best transfection efficiency were selected to further prepare CP30Dc and CP70Dc.

3.1.2. SDS-PAGE. SDS-PAGE analysis was performed to verify the successful preparation of CPDc. As shown in Figure 3a, all bands of the 293T cell membrane extract (lane 4) were consistent with those of the 293T cell suspension (lane 2). However, the bands of the 293T-CM extract were not as rich as those of the 293T cell suspension due to protein loss during extraction. PEI70k/DNA did not show a band (lane 5) in the SDS-PAGE assay but presented the same electrophoretic band as the 293T cell membrane when it was encapsulated by the CM form 293T-CP70Dc (lane 3). Similarly, as shown in Figure 3b, the SDS-PAGE results of HepG2-CP70Dc and HeLa-CP70Dc showed that most of the protein of the HepG2 and HeLa-CM was detected in the CP70Dc, which indicated that these CPDcs were successfully prepared by CM coating onto the PEI70/DNA complex.

3.1.3. Morphology of CPDc. The TEM results of CP70Dc are shown in Figure 3c. The PEI/DNA complex was an irregular spherical particle with a diameter of about 50−260 nm. The particle size of CPDc was about 200 nm, which was consistent with the DLS results. The surface of the PEI/DNA complex was covered with a CM coating with a thickness of about 6−10 nm. There was no significant difference in the morphology of CP70Dcs prepared by different CM packages, which might be due to the same preparation method. However, due to the adhesion between the cell membranes, CP70Dcs adhered to each other. Hence, the single CP70Dc could not be observed from the TEM results, and their size was not uniform. This might be overcome by reducing the dispersion concentration of CP70Dc.

3.1.4. EE of CPDc. The effective encapsulation of PEI/DNA by the CM is the guarantee for the preparation of CPDc as an efficient gene carrier. Therefore, the effects of the mass ratio and extrusion times on the EE were investigated, and the optimal mass ratio and extrusion times were determined. As shown in Figure 2e,f, the EE of the two kinds of capsules first increased and then decreased with the increase in the mass ratio. 293T-CP70Dc showed a highest EE of 72.3% at a mass ratio of 2/2.5/1, which exhibited no significant change with the increase of extrusion times (Figure 3d). 293T-CP70Dc showed a highest EE of approximately 83.5% at a mass ratio of 2/0.75/1 and 15 extrusion times (Figure 3e). This parameter increased and then decreased with the extrusion times. On the basis of these results, the parameters for optimal CPD preparation were as follows: the mass ratios of 293T-CP30Dc and 293T-CP70Dc were 2/2.5/1 and 2/0.75/1, respectively, and the extrusion times were 15 times.

3.1.5. DLS and ζ-Potential. The particle size and ζ-potential of CPDcs with different mass ratios were analyzed using a nanoparticle size analyzer. As shown in Figure 3f, the particle size of the PEI30k/DNA complex was about 210 nm, and the particle size of the 293T-CM fragment was about 425 nm. The particle size of CP30Dc was larger than that of the PEI/DNA complex but smaller than that of the 293T-CM fragment. When the mass ratio was 0.5/2.5/1 to 4/2.5/1, the particle size of CP30Dc was about 220−225 nm, and there was no significant difference in the particle size of 293T-CP30Dc with different mass ratios. As shown in Figure 3g, the particle size of PEI70/DNA was about 265 nm, which was larger than PEI30/DNA. Compared with 293T-CP30Dc, the particle size of 293T-CP70Dcs with different mass ratios only increased slightly, and the particle size was the smallest at 2/0.75/1, about 225 nm. This might be due to the larger size of the PEI70/DNA complex. As shown in Figure 3i, although the particle size of HepG2 and HeLa-CM fragments were larger than the 293T-CM, the size of HepG2-CP70Dc and HeLa-CP70Dc were similar to 293T-CPDc. These results indicated that the size of the PEI/DNA complex was relatively uniform after CM encapsulation by liposome extrusion. In addition, the size of HeLa-CP70Dc was significantly larger than that of HepG2-CP70Dc, which might be due to the fact that the size of the HeLa-CM fragment was larger than that of HepG2. As shown in Figure 3f, the ζ-potential of the PEI30k/DNA complex was about +18, which was caused by the positive charge of PEI. The ζ-potential of the 293T-CM was negative (−15) because of its negative phospholipid. With the increase of the mass ratio from 0.5/2.5/1 to 4/2.5/1 293T-CP30Dc,

https://doi.org/10.1021/acs.molpharmaceut.1c00359
Mol. Pharmaceutics 2021, 18, 2803−2822

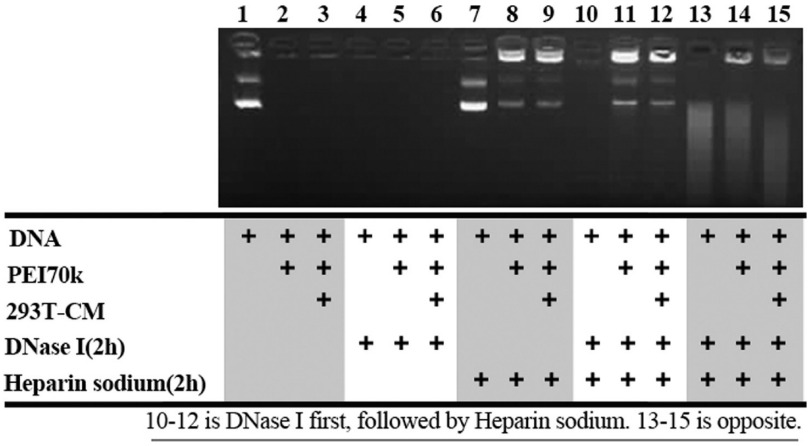

Figure 4. Gel electrophoresis results of DNA condensation and protection ability of 293T-CP70Dc.

the ζ-potential decreased from +15 to −8. This indicates that the 293T-CM was successfully coated on the PEI30/DNA complex, and then the positive charge of the PEI/DNA complex was neutralized by the negative charge of the CM. As shown in Figure 3h, PEI70/DNA shows a strong positive charge of +22, which was due to the rich amino of PEI70k. The change of the ζ-potential of 293T-CP70Dc was similar to that of 293T-CP30Dc, that is, it decreased with the increase of the mass ratio. However, unlike 293T-CP30Dc, due to the strong positive charge of PEI7MP0k, 293T-CP70Dc was close to neutral when the mass ratio was 4/2.5/1, which was higher than −8 of 293T-CP30Dc. The above trend was also applicable to HepG2-CP70Dc and HeLa-CP70Dc. After being embedded by HepG2-CM and HeLa-CM, the ζ-potential of the PEI70/DNA complex decreased significantly (Figure 3h). These results indicated that CM encapsulation could reduce the positive charge of the PEI/DNA complex effectively and might reduce its cytotoxicity. In addition, it should be noted that the CPDc in this study was prepared by the liposome extrusion method, and the mixture of the PEI/DNA complex and the CM was extruded through a microporous membrane with a pore size of 200 nm. Therefore, the particle size of the PEI/DNA complex did not change significantly after CM encapsulation. However, due to the negative charge of the CM, the ζ-potential of the CPDc surface gradually decreased or even changed to negative with the increase of the CM mass ratio in CPDc. As shown in Figure 3i, the particle size of each ECM was about 70−110 nm, which was smaller than that of the CM. The particle size of ECM-CP70Dcs was close to that of various CP70Dcs, indicating that the particle size of CP70Dcs did not increase significantly after adding the ECM, which might be due to the small size of the ECM and the same preparation method. According to the ζ-potential results (Figure 3h), all kinds of ECMs show a positive ζ-potential, which led to the increase of the ζ-potential of CP70Dc after ECM doping.

3.2. DNA Protection and Release. Numbers of enzymes and other biological macromolecules such as nuclease are dissociated inside and outside cells, which is a great threat to DNA delivery in vivo. Therefore, the success of cell transfection depends on whether the DNA is not hydrolyzed by nuclease and is successfully released at a specific location to perform the next step of transport and even complete transcription and translation. Agarose gel electrophoresis was used to explore the protective and releasing ability of CPDc for DNA. As shown in Figure 4, the band of naked DNA (lane 1) was visible. The PEI70k/DNA complex (lane 2) and CPDc (lane 3) were all blocked in the loading well. Hence, no visible band was observed, implying the lack of free DNA in both samples. After incubation with DNase I, no visible bands were found in the naked DNA, PEI70k/DNA complex (lane 5), and CPDc (lane 6). Therefore, the hydrolysis of DNA was impossible to determine. In the presence of Active Ingredient sodium, the PEI70k/DNA complex (lane 8) and CPDc (lane 9) showed the same bands as naked DNA. This finding implied that these capsules could release free DNA effectively, which was important for DNA release and further transfection after the complexes entered cells. The protective effect of CPDc on DNA was further verified by DNase I treatment, followed by Active Ingredient sodium. The results showed that the naked DNA (lane 10) was hydrolyzed by nuclease, and the PEI70k/DNA complexes (lane 11) and CPDc (lane 12) still had the same band as that of naked DNA for control. This phenomenon occurred because the DNA in the PEI/DNA complex and CPDc was not hydrolyzed by nuclease and instead was successfully replaced and released after the Active Ingredient sodium was added. On the contrary, when the Active Ingredient sodium was added and then treated with nuclease, the released DNA was hydrolyzed by nuclease (lanes 14 and 15). These results confirmed that the CPDc complex had the ability to protect the DNA from being hydrolyzed by nuclease.

3.3. Cell Uptake of CPDc. The uptake of 293T-CPDc in 293T cells was observed by CLSM. As shown in Figures 5 and 6, blue indicates DAPI-labeled nucleus, green indicates FITC-labeled different vector/DNA complexes or CPDcs, and red fluorescence indicates Dil-labeled 293T cell membrane. All images were processed by merger to analyze the cell uptake and the relative position of CPDc. Figures 5a and 6a show that PEI30k/DNA (2.5/1) and PEI70k/DNA (0.75/1) complexes could be ingested by cells. When the mass ratio of 293T-CP30Dc (Figure 5a) was 2/2.5/1, 293T-CP70Dc (Figure 6a) and nucleus overlapped the most, indicating that 293T-CP70Dc had the highest cell uptake efficiency at this mass ratio. As shown in Figure 6a, the uptake efficiency of 293T-CP70Dc increased with the mass ratio. 293T-CP70Dc aggregated near the nucleus, indicating its higher cell uptake efficiency compared with the PEI70k/DNA complex. Moreover, the Dil-labeled cell membrane was almost completely wrapped around the nucleus during cell ingestion, implying that the uptake mode of 293T-CP70Dc might be membrane

https://doi.org/10.1021/acs.molpharmaceut.1c00359
Mol. Pharmaceutics 2021, 18, 2803−2822

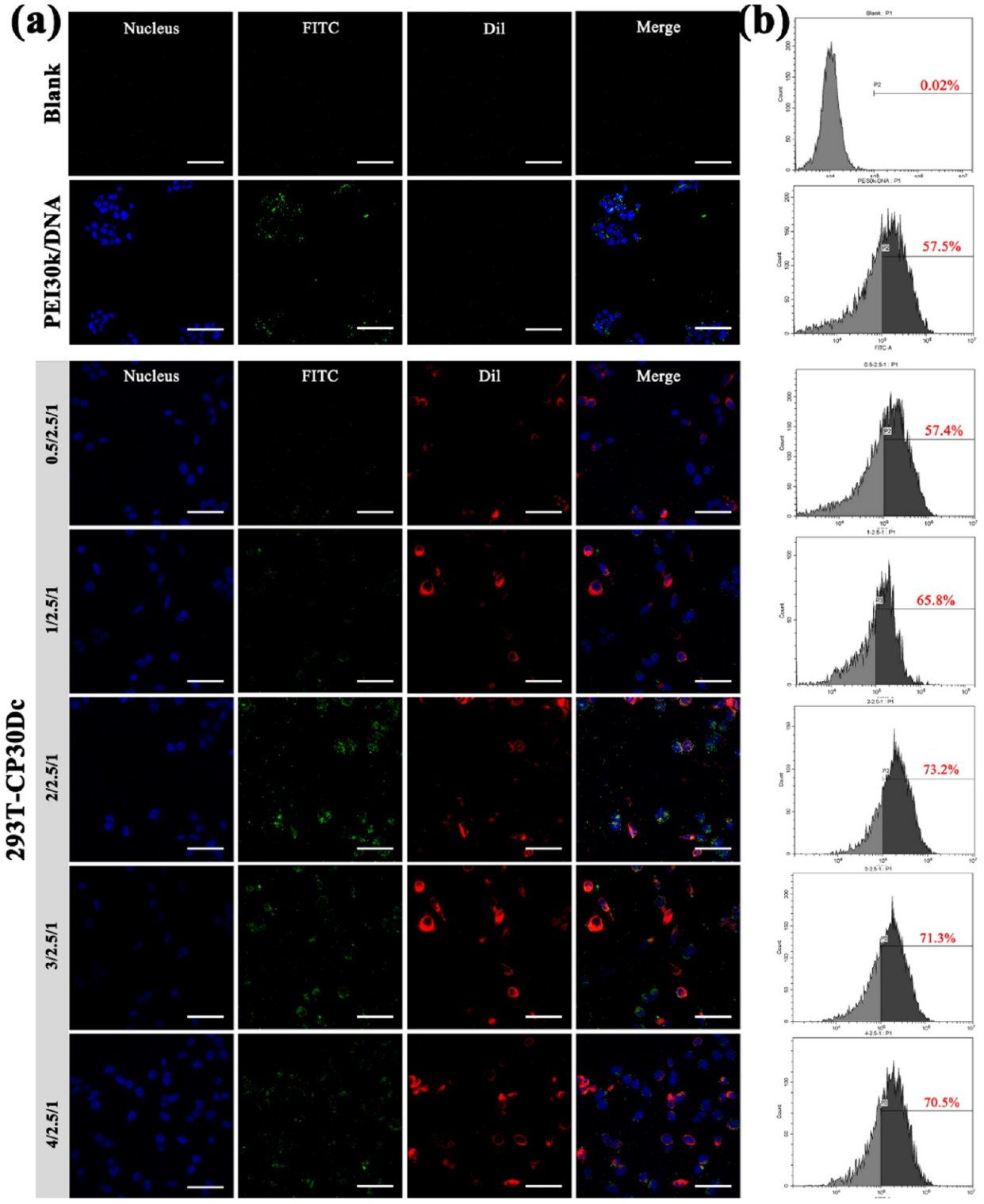

Figure 5. Cell uptake results of 293T-CP30Dc. (a) Confocal microscopy images (400×) of intracellular trafficking of the FITC-labeled PEI/DNA complexes and CP30Dcs in 293T cells. (red: Dil-labeled cell membrane; blue: DAPI-stained cell nuclei; Green: FITC-labeled PEI), (Scale bar = 50 μm). (b) Flow cytometry results of cell uptake efficiency of various 293T-CP30Dcs.

fusion. Flow cytometry results (Figures 5b and 6b) show that the cell uptake rate of 293T-CP30Dc was gradually increased with the mass ratio. Its highest efficiency of 75% was obtained at a mass ratio of 2/2.5/1, which was approximately 20% higher than that of the PEI30k/DNA complex, and then slowly decreased. Figure 6b shows that with the increase in the mass ratio, the cell uptake of 293T-CP70Dc first increased and then leveled off. Its highest cell uptake efficiency of approximately 92% was attained at a mass ratio of 2/0.75/1, which was approximately 15% higher than that of the PEI70k/DNA complex.

3.4. In Vitro Gene Transfection of 293T-CPD. Transfection is one of the most important properties of gene vectors. The EGFP plasmid was used as a reporter gene to investigate

https://doi.org/10.1021/acs.molpharmaceut.1c00359
Mol. Pharmaceutics 2021, 18, 2803−2822

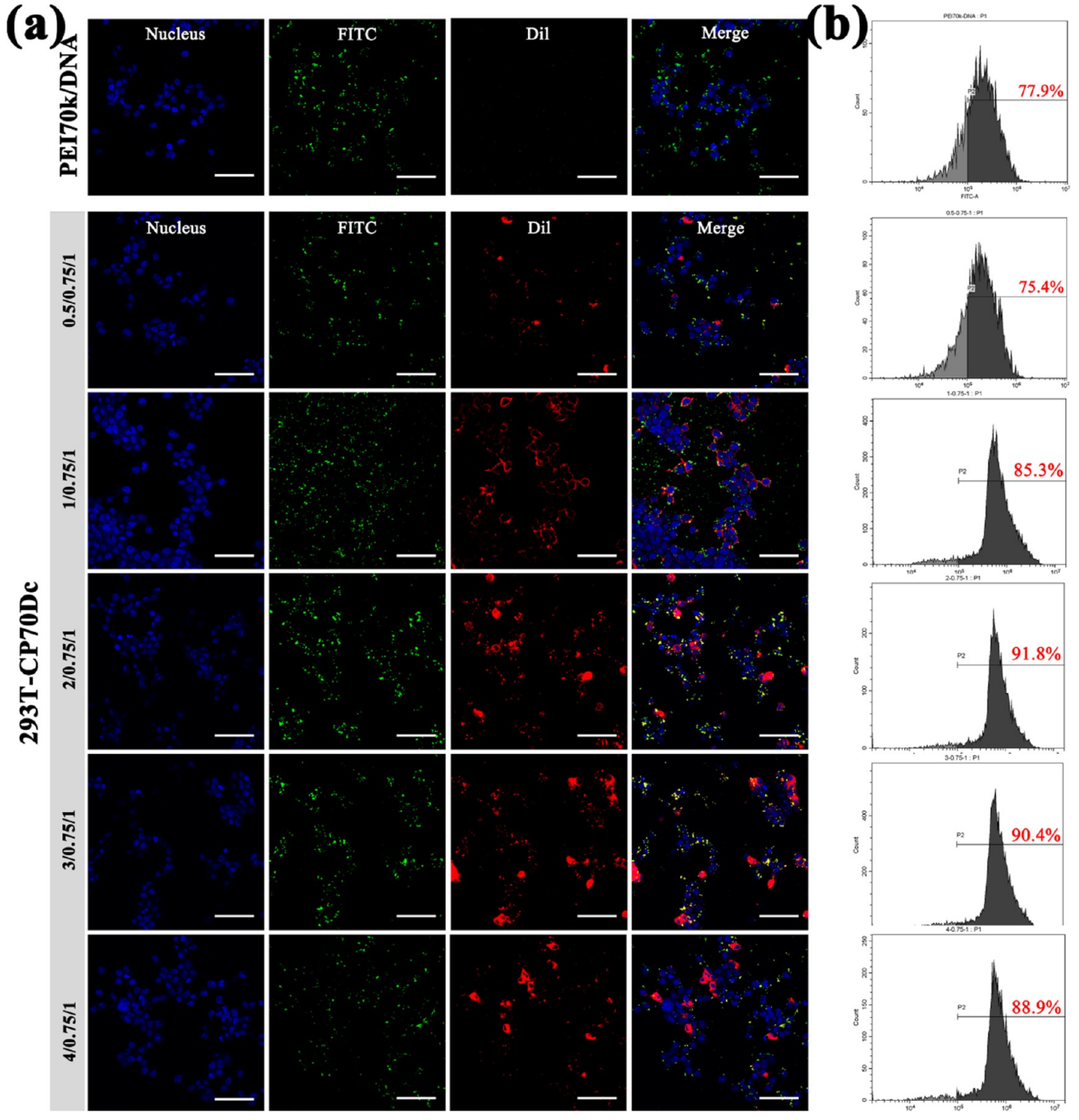

Figure 6. Cell uptake results of 293T-CP70Dc. (a) Confocal microscopy images (400×) of intracellular trafficking of the FITC-labeled PEI/DNA complexes and CP70Dcs in 293T cells. (red: Dil-labeled cell membrane; blue: DAPI-stained cell nuclei; Green: FITC-labeled PEI), (Scale bar = 50 μm). (b) Flow cytometry results of the cell uptake efficiency of various 293T-CP70Dcs.

the gene transfection efficiency of 293T-CPDc in 293T cells. As shown in Figure 7a, various 293T-CPDcs were released DNA into 293T cells and successfully expressed the green fluorescent protein. The abundance of the green fluorescent protein reflected the transfection efficiency of two different capsules. At different mass ratios, the transfection efficiency of 293T-CP70Dc (Figure 7b) was higher than that of 293T-CP30Dc. This finding was consistent with the trend of cell uptake efficiency, suggesting that high uptake efficiency was the prerequisite for obtaining high transfection efficiency. As shown in Figure 4a, the transfection efficiency of 293T-CP30Dc at different mass ratios was not significantly improved compared with that of the PEI30k/DNA complex. This result was consistent with the flow cytometry analysis (Figure 7c,d), that is, the transfection efficiency of 293T-CP30Dc at different mass ratios was equivalent to that of the PEI30k/DNA complex. As shown in Figure 7c–h, the transfection efficiency of 293T-CP70Dc was slightly higher than that of the PEI70k/DNA complex at high mass ratios. When the mass ratio was 2/0.75/1, the transfection efficiency of 293T-CP70Dc was approximately 76%, which was 10% higher than that of the PEI70k/DNA complex. At other mass ratios, the transfection

https://doi.org/10.1021/acs.molpharmaceut.1c00359
Mol. Pharmaceutics 2021, 18, 2803−2822

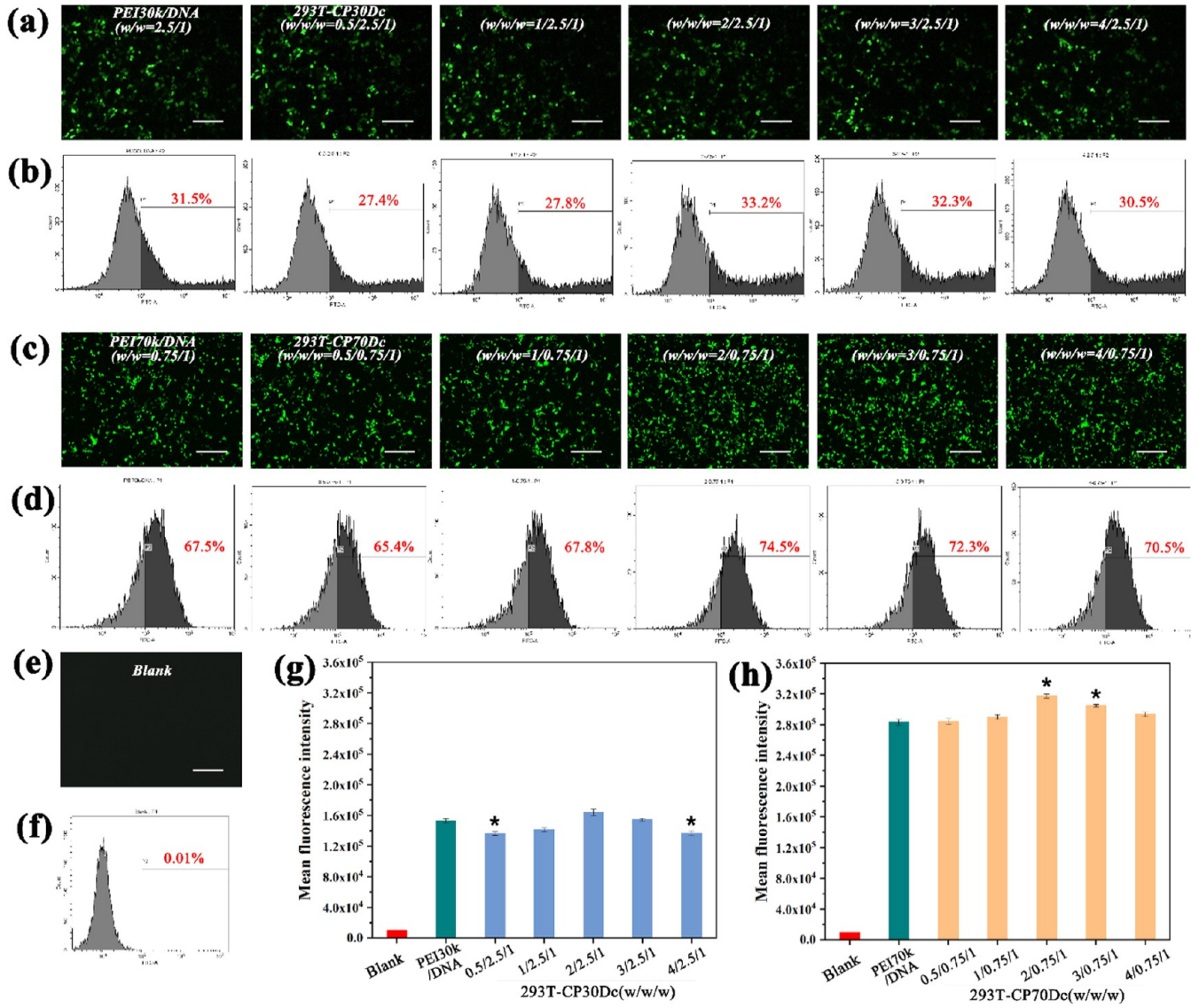

Figure 7. Gene transfection results of 293T-CP30Dc and 293T-CP70Dc in 293T cells. (a) Fluorescence microscopy images (40×) of positive EGFP expression 293T cells treated with 293T-CP30Dc (Scale bar = 1000 μm). (b) Flow cytometry results of gene transfection of 293T-CP30Dc in 293T cells. (c) Fluorescence microscopy images (40×) of positive GFP expression 293T cells treated with 293T-CP70Dc. (Scale bar = 1000 μm). (d) Flow cytometry results of gene transfection of 293T-CP70Dc in 293T cells. (e) Mean fluorescence intensity of positive EGFP expression 293T cells treated with 293T-CP30Dc. (f) Mean fluorescence intensity of positive EGFP expression 293T cells treated with 293T-CP70Dc. (g) Mean fluorescence intensity of 293T cells transfected with 293T-CP30Dcs. (h) Mean fluorescence intensity of 293T cells transfected with 293T-CP70Dcs. (mean ± SD, n = 3, *$p \leq 0.05$).

efficiency of 293T-CP70Dc was slightly improved. This phenomenon might be due to the highest EE and small particle size of 293T-CP70Dc at a mass ratio of 2/0.75/1.

3.5. Targeting Effect of CP70D. *3.5.1. Cell Uptake of CP70Dcs.* The uptake efficiency and transfection efficiency in different cells were analyzed for CPDcs prepared with different cell membranes to further study and confirm their targeting. All CPDcs, including HeLa and HepG2-CM-encapsulated capsules, HeLa-CP70Dc, and HepG2-CP70Dc, were prepared with PEI70k according to the method for 293T-CP70Dc with a mass ratio of 2/0.75/1 in Section 2.3. Figure 8a shows that compared with the other CPDcs, 293T-CP70Dc with green fluorescence showed the highest cell uptake efficiency in 293T cells. Similarly, HepG2-CP70Dc had the highest uptake efficiency in HepG2 cells, and HeLa-CP70Dc exhibited higher cell uptake efficiency than other CPDcs. As shown in Figure 8b, confocal microscopy images show that various CP70Dcs (green) could be successfully transferred to the cells after incubating with 293T, HepG2, and HeLa cells and distributed around or inside the nucleus (blue). Flow cytometry results (Figure 8c) showed that in 293T cells, the cellular uptake efficiency of 293T-CP70Dc was approximately 92%, which was higher than that of the other two capsules. In HepG2 cells, the uptake efficiency of HepG2-CP70Dc was approximately 55%, which was higher than that of the other two capsules. All CPDcs showed low transfection efficiency, but HeLa-CP70Dc showed a cell uptake efficiency of approximately 35%, which was higher than those of other CPDcs. These results suggested that various CPDcs prepared with different CMs exhibited cell homology targeting during their cell uptake. The results suggested that the transfection efficiency of three kinds of CPDcs in 293T cells was higher than that in the same original

https://doi.org/10.1021/acs.molpharmaceut.1c00359
Mol. Pharmaceutics 2021, 18, 2803−2822

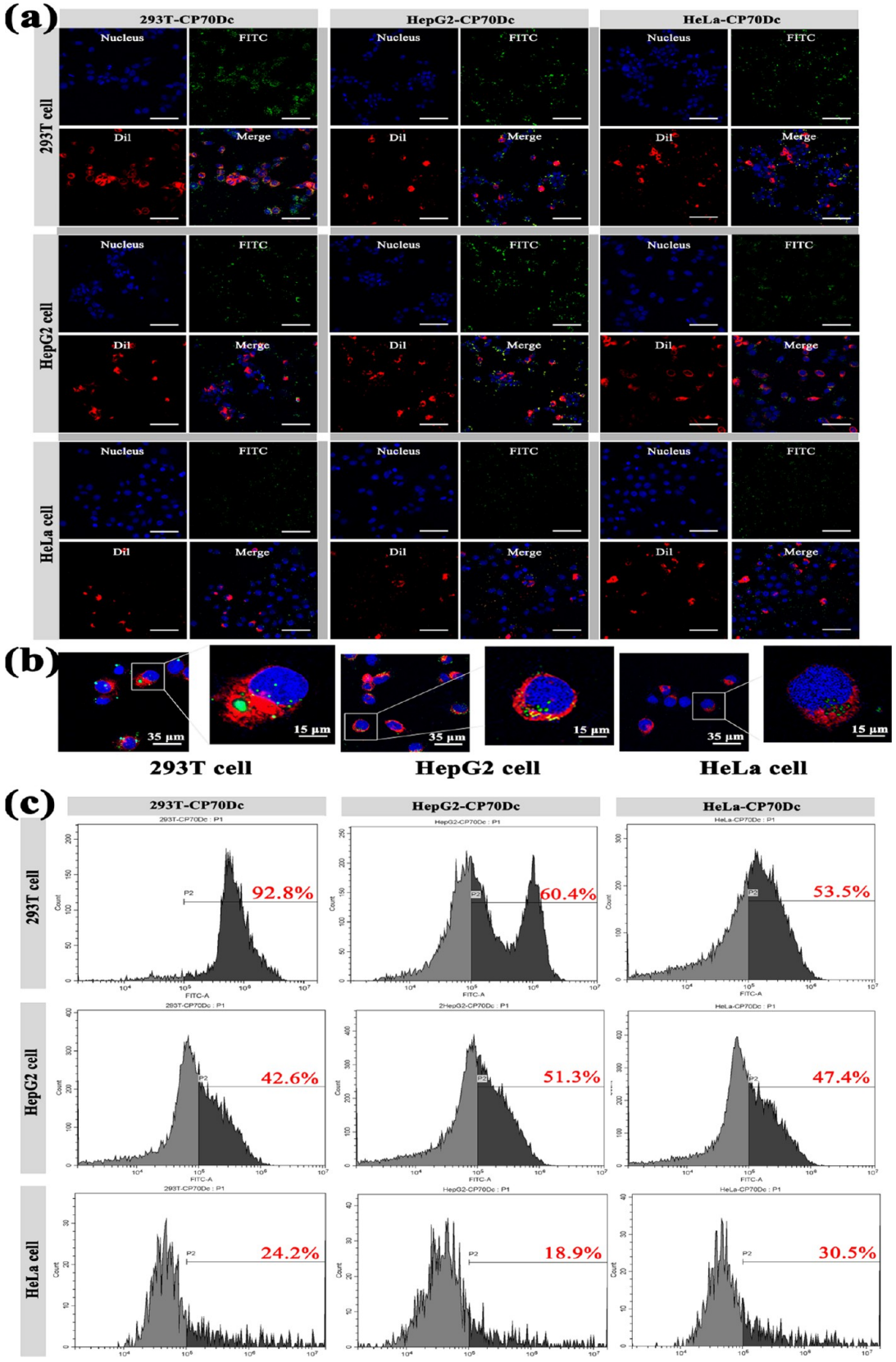

Figure 8. Cell uptake of various CP70Dcs. (a) Confocal microscopy images (400×) of intracellular trafficking of 293T-CP70Dc, HepG2-CP70Dc, and HeLa-CP70Dc in 293T, HepG2, and HeLa cells, respectively. (red: Dil-labeled cell membrane, blue: DAPI-stained cell nuclei, Green: FITC-labeled PEI), (Scale bar = 35, 15 μm). (b) Confocal microscopy images (600× and 1000×) of intracellular trafficking of 293T-CP70Dc in 293T, HepG2, and HeLa cells. (c) Flow cytometry results of cell uptake of various CP70Dcs.

https://doi.org/10.1021/acs.molpharmaceut.1c00359
Mol. Pharmaceutics 2021, 18, 2803−2822

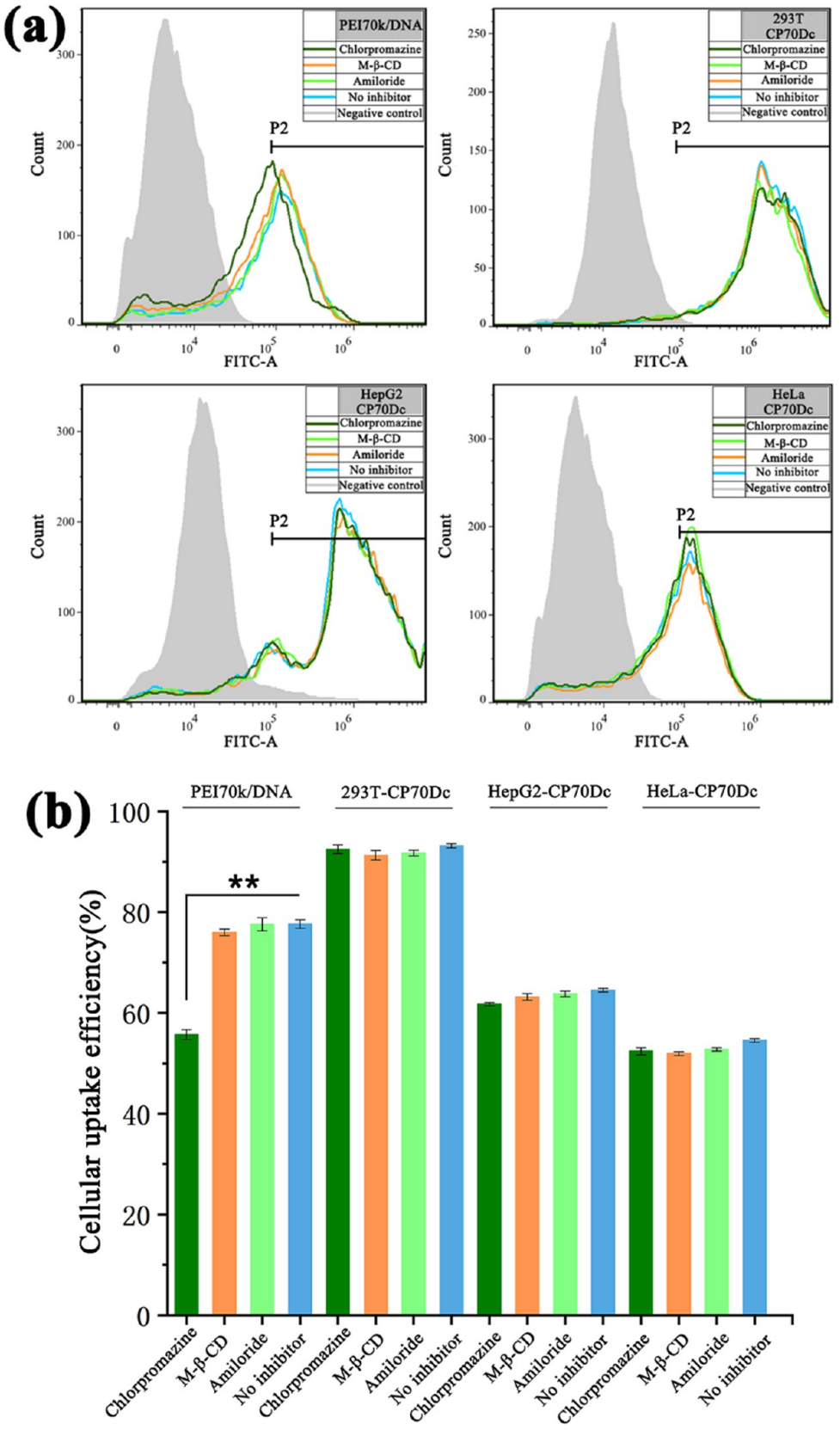

Figure 9. Cell uptake efficiency of various CP70Dcs in 293T cells under the intervention of transport inhibitors. (a) Cell uptake efficiency of various CP70Dcs under inhibition of no inhibitor, Active Ingredient (0.03 mmol/mL), methyl-β-cyclodextrin (10 mmol/L), and Active Ingredient (2.5 mmol/L) measured by flow cytometry. (b) Cell uptake efficiency of various CP70Dcs under inhibition of different inhibitors, compared to no inhibitor. (*$p < 0.05$, **$p < 0.01$).

https://doi.org/10.1021/acs.molpharmaceut.1c00359
Mol. Pharmaceutics 2021, 18, 2803−2822

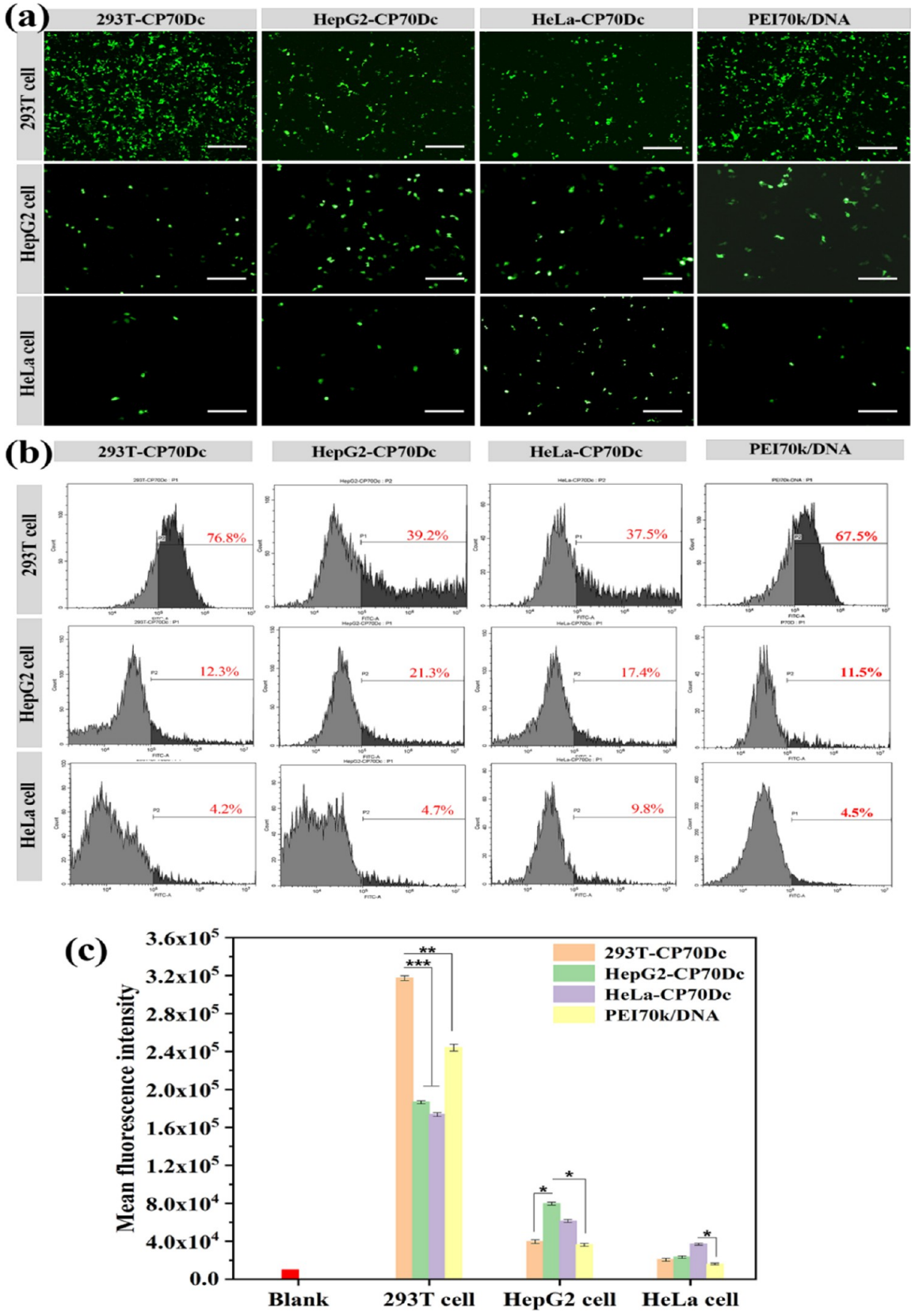

Figure 10. Gene transfection results of 293T-CP70Dc in 293T, HepG2, and HeLa cells. (a) Fluorescence microscopy images (40×) of positive EGFP expression cells treated with 293T-CP30Dc (Scale bar = 1000 μm). (b) Flow cytometry results of gene transfection of 293T-CP70Dc in various cells. (c) Mean fluorescence intensity of positive EGFP expression 293T cells treated with various CP70Dcs. (mean ± SD, $n = 3$, $^{*}p \leq 0.05$, $^{**}p \leq 0.01$, $^{***}p \leq 0.0005$).

https://doi.org/10.1021/acs.molpharmaceut.1c00359
Mol. Pharmaceutics 2021, 18, 2803−2822

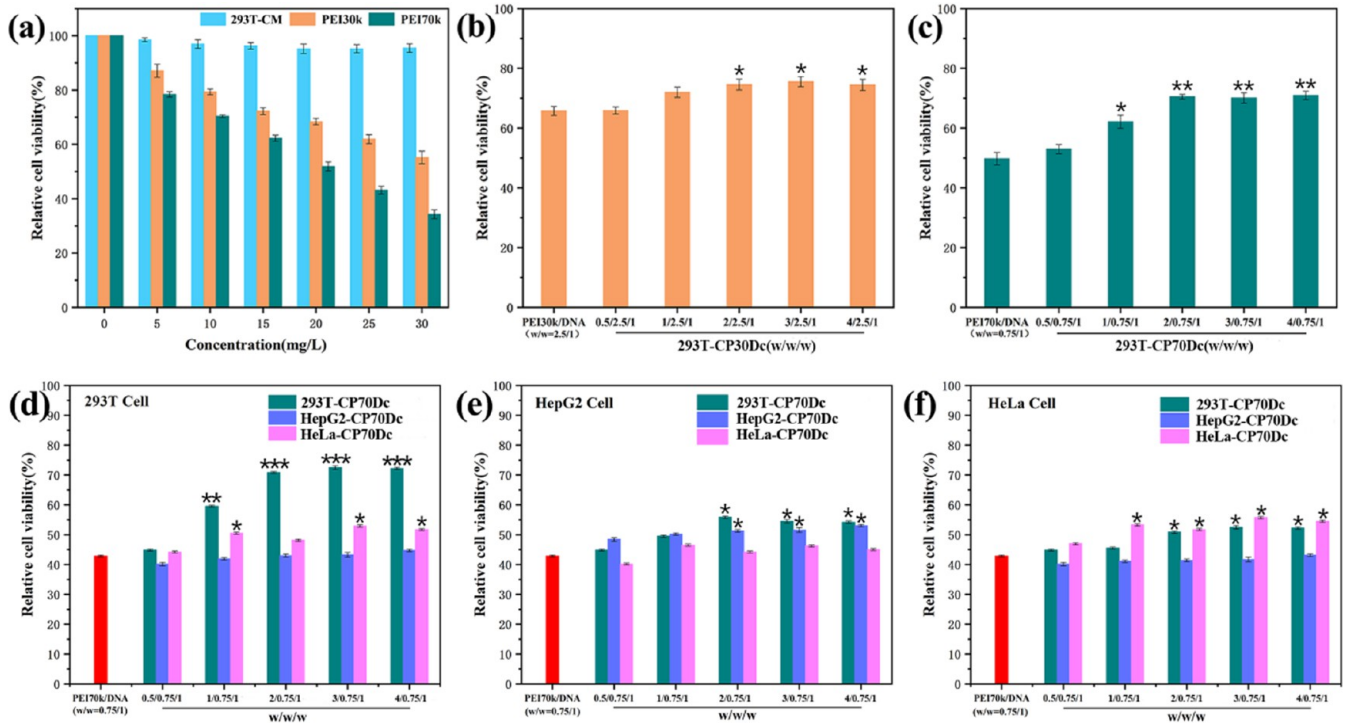

Figure 11. Cell viability assay of various cells treated with different vectors and vector/DNA polyplexes under different concentrations and mass ratios. (a) Cell viability of 293T cells treated with 293T-CM, PEI30k, and PEI70k. (b) Cell viability of 293T cells treated with 293T-CP30Dc. (c) Cell viability of 293T cells treated with 293T-CP70kDc. (d) Cell viability of 293T cells treated with 293T-CP70Dc, HepG2-CP70Dc, and HeLa-CP70Dc. (e) Cell viability of HepG2 cells treated with 293T-CP70Dc, HepG2-CP70Dc, and HeLa-CP70Dc. (f) Cell viability of HeLa cells treated with 293T-CP70Dc, HepG2-CP70Dc, and HeLa-CP70Dc. (mean ± SD, $n = 3$, $^{*}p \leq 0.05$, $^{**}p \leq 0.001$, $^{***}p \leq 0.0005$).

cells, although CPDcs coated with different cell membranes showed obvious homologous targeting. This might be determined by the particularity of the 293T cells because it was a cell line expressing SV40 virus T antigen, which was derived from human embryonic kidney cell 293HEK. After modification, T antigen is inserted into 293T cells, so a foreign gene material can exhibit a higher expression level in 293T cells. It also suggests that the preparation process of CPDc needs to further optimize for higher transfection efficiency, such as quantifying the cell membrane of CPDc, more uniform particle size, and so on. In addition, it implied that more attention should be paid to the universality of gene vectors in different cells in further research.

3.5.2. Cell Uptake Pathway of CP70Dc. The effects of different transport inhibitors on the uptake efficiency of CPDc in 293T cells were studied. The uptake efficiency of CPDc without the cell transport inhibitor in 293T cells was used as a positive control group. As shown in Figure 9, the uptake efficiency of the PEI/DNA complex in 293T cells treated with Active Ingredient decreased significantly ($p < 0.001$), while the uptake efficiency of the PEI/DNA complex in 293T cells treated with methyl β-cyclodextrin and Active Ingredient did not differ from that in the noninhibitor group, indicating that the PEI/DNA complex might enter the cells through clathrin-dependent endocytosis. For 293T-CP70Dc, HepG2-CP70Dc, and HeLa-CP70Dc, there was no significant change in cell uptake efficiency after treatment with three inhibitors. These results suggested that CP70Dc might not enter the cells through three typical pathways: clathrin-dependent endocytosis, caveolin-dependent endocytosis, or macrosomia. It also meant that cell membrane encapsulation might change the pathway of the PEI/DNA complex into cells, which was consistent with the literature report, that is, the cell membrane-encapsulated complex was more likely to enter cells through membrane fusion.

3.5.3. In Vitro Gene Transfection of CP70Dcs. The targeting of CP70Dc was studied by gene transfection in vitro. As shown in Figure 10, EGFP (green fluorescence) was observed in all three kinds of cells treated with various CP70Dcs, but the transfection efficiency in 293T cells was significantly higher than that in the other two kinds of cells. As shown in Figure 10a, the transfection efficiency of 293T-CP70Dc in 293T cells was higher than those of HepG2-CP70Dc and HeLa-CP70Dc. The transfection efficiency of HepG2-CP70Dc and HeLa-CP70Dc in homologous cells of the CM was relatively high. As confirmed by flow cytometry, these findings suggested that different CP70Dcs had homologous cell membrane targeting. Figure 10b,c shows that in 293T cells, the transfection efficiency of 293T-CP70Dc was 76%, which was approximately 35% higher than that of the other two capsules. In HepG2 cells, the transfection efficiency of HepG2-CP70Dc was the highest at approximately 23%, which was higher than that of the other two capsules. In HeLa cells, the transfection efficiency of the three capsules was lower than 20%, but that of HeLa-CP70Dc was significantly higher than those of the other two CP70Dcs. These results were consistent with the cell uptake efficiency of different CP70Dcs.

3.6. Cytotoxicity. As an essential feature of a safe gene vector, cytotoxicity affects the transfection efficiency of the gene directly. Therefore, the cytotoxicity of different CPDcs was studied by the MTT assay to evaluate their safety as a gene vector. As shown in Figure 11a, the 293T-CM did not show significant cytotoxicity because the cell survival rate under this treatment was more than 98%. However, PEI30k and PEI70k

https://doi.org/10.1021/acs.molpharmaceut.1c00359
Mol. Pharmaceutics 2021, 18, 2803−2822

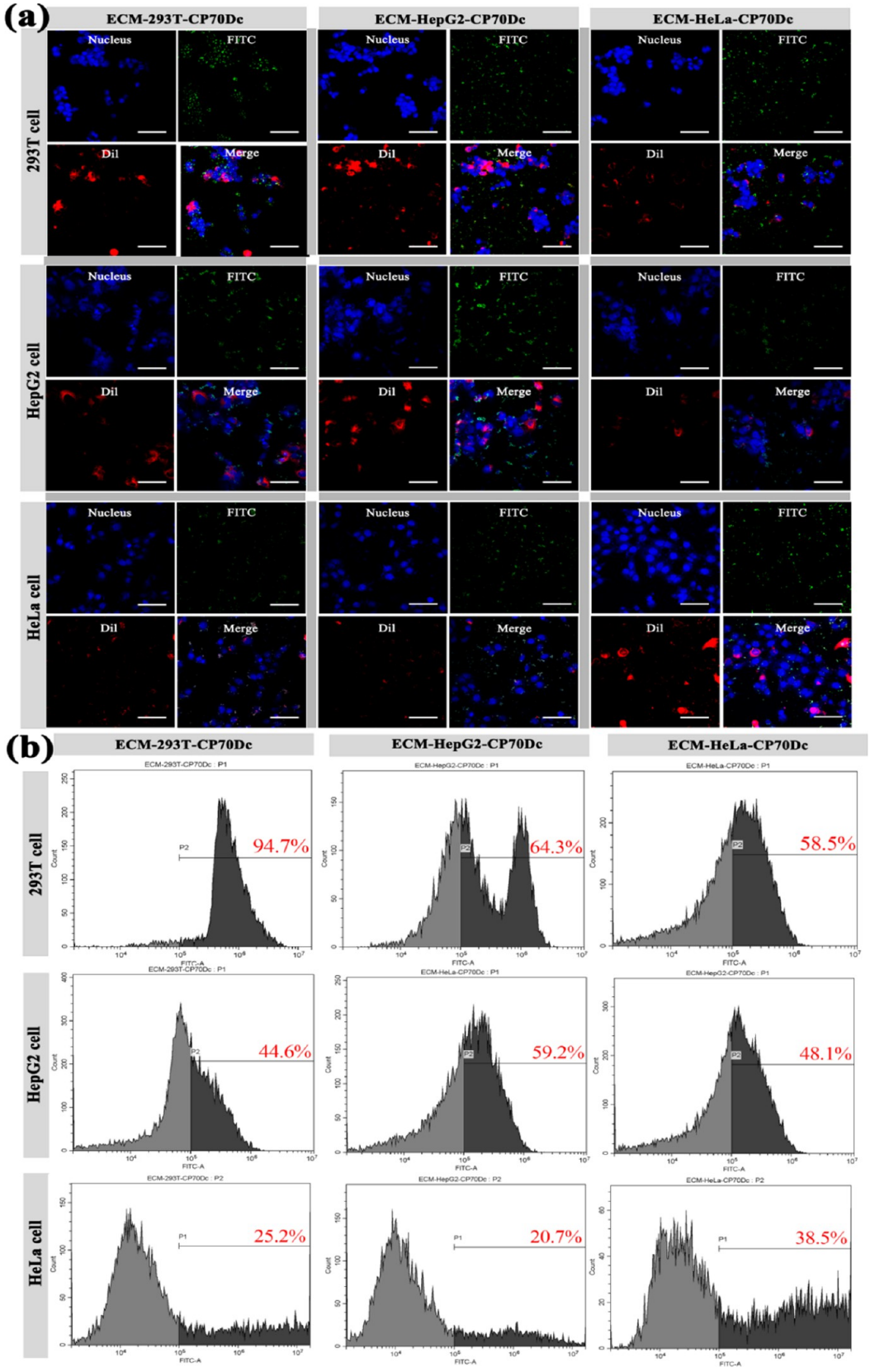

Figure 12. Cell uptake of various ECM-CP70Dc. (a) Confocal microscopy images (400×) of intracellular trafficking of ECM-293T-CP70Dc, ECM-HepG2-CP70Dc, and ECM-HeLa-CP70Dc in 293T, HepG2, and HeLa cells, respectively. (red: Dil-labeled cell membrane, blue: DAPI-stained cell nuclei, Green: FITC-labeled PEI), (Scale bar = 100 μm). (b) Flow cytometry results of cell uptake of various ECM-CP70Dcs.

showed cytotoxicity with the increasing concentration, suggesting that the safety of naked PEI was poor. Figure 11b,c shows that compared with those cocultured with PEI30k/DNA, the cells cocultured with CP30Dc and

https://doi.org/10.1021/acs.molpharmaceut.1c00359
Mol. Pharmaceutics 2021, 18, 2803−2822

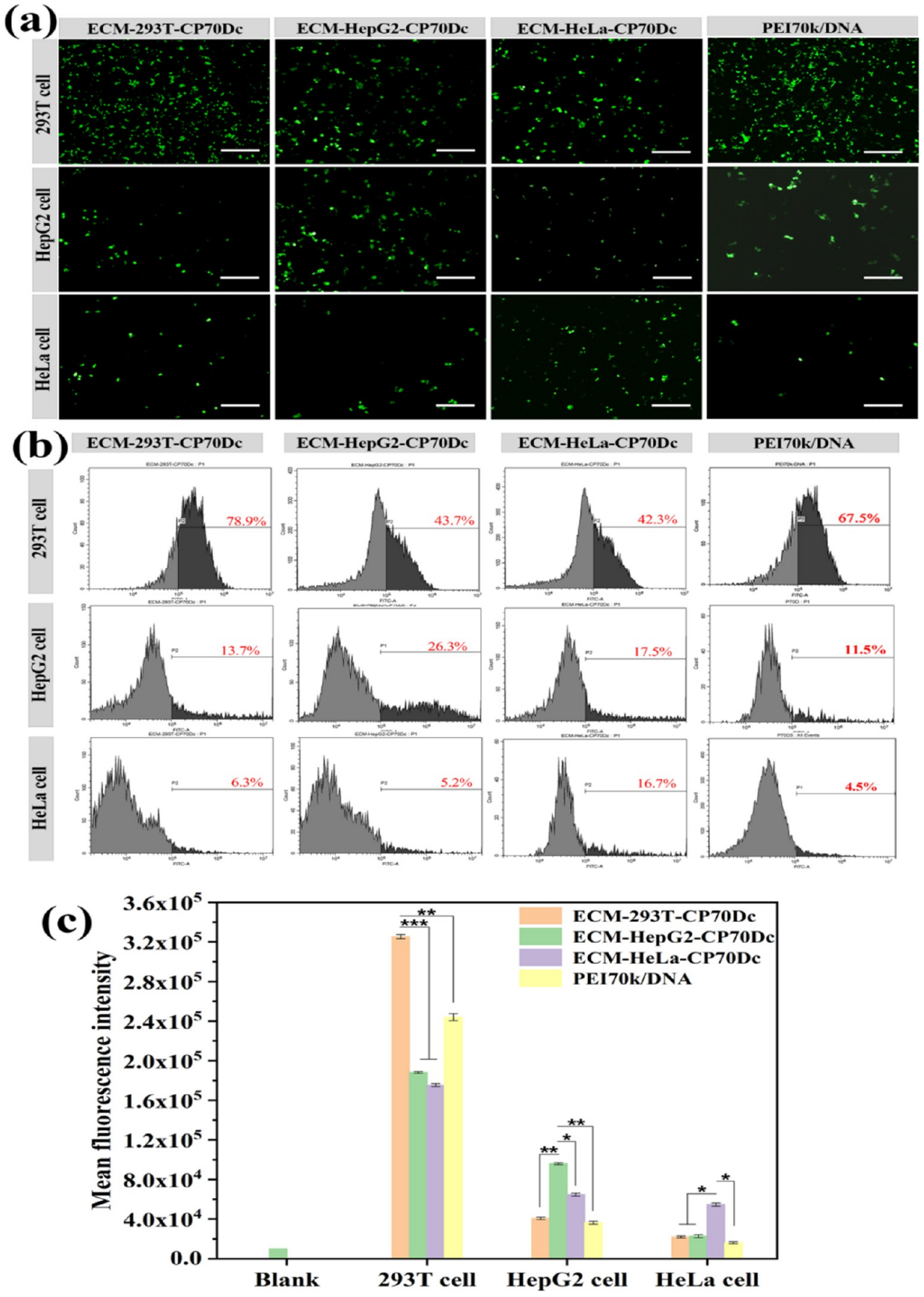

Figure 13. Gene transfection results of various ECM-CP70Dc in 293T, HepG2, and HeLa cells. (a) Fluorescence microscopy images (40×) of positive EGFP expression cells treated with various ECM-CP70Dcs. (Scale bar = 1000 μm). (b) Flow cytometry results of gene transfection of ECM-CP70Dc in various cells. (c) Mean fluorescence intensity of positive EGFP expression 293T cells treated with various ECM-CP70Dcs. (c) Mean fluorescence intensity of gene transfection of ECM-CP70Dc in various cells (mean ± SD, n = 3, *$p \leq 0.05$, **$p \leq 0.01$, **$p \leq 0.0005$).

https://doi.org/10.1021/acs.molpharmaceut.1c00359
Mol. Pharmaceutics 2021, 18, 2803−2822

CP70Dc exhibited gradually increasing viability with the cell membrane mass ratio. This parameter reached the highest when the mass ratios were 2/2.5/1 and 1/0.75/1, which were significantly higher than that of PEI/DNA complexes with the same mass ratios. In particular, the cell viability of 293T-CP70Dc-treated cells was higher than that of PEI70k/DNA-treated cells, approximately 20%. These results suggested that cell membrane encapsulation could effectively reduce the cytotoxicity of the PEI/DNA complex.

The cell viability of CPDcs prepared by different CMs was analyzed. The results showed that with the increase in the mass ratio, the cell viability of 293T-CP70Dc-treated cells gradually increased with the mass ratio in 293T cells (Figure 11d) and stabilized when the mass ratio was 2/0.75/1. The cell viability of HepG2-CP70Dc and HeLa-CP70Dc-treated cells did not increase significantly compared with that of PEI70k/DNA-treated cells. In HepG2 cells (Figure 11e), the cell viability of cells cocultured with 293T-CP70Dc or HepG2-CP70Dc increased slightly with the increase of the mass ratio, and that of the HepG2-CP70Dc of HepG2 cells cocultured with HeLa-CP70Dc was lower than that of other CPDcs. In HeLa cells (Figure 11f), the cell viability of cells cocultured with HeLa-CP70Dc increased with the increase of the mass ratio and was higher than that of other CP70Dcs. The cell viability of cells cocultured with HepG2-CP70Dc was lower than that of the PEI70k/DNA complex. The cell viability of cells cocultured with 293T-CP70Dc increased with the increase of the mass ratio. These results indicated that the cytotoxicity of the PEI/DNA complex was effectively reduced by cell membrane encapsulation. In addition, homologous CPDcs showed high safety and even promoted cell proliferation, but heterologous CPDcs did not substantially reduce the cytotoxicity of the PEI/DNA complex.

3.7. Targeting Effect of ECM-CPDc. *3.7.1. Cell Uptake of ECM-CPDc.* The ECM can remarkably promote the adhesion of CPDc to cells, possibly enhance the adhesion between CPDcs and cells, and consequently improve the uptake and transfection efficiency of CPDc. The analysis results of the cell uptake of ECM-CP70Dc are shown in Figure 12a. All ECM-CP70Dcs could be ingested by cells. The aggregation degree of green fluorescence around the homologous nucleus was significantly stronger than that around the nonhomologous cells. This finding indicated that ECM-CP70Dc had homologous targeting, which was enhanced compared with that of CP70Dcs, especially ECM-293T-CP70Dc. Flow cytometry results (Figure 12b) confirmed this conclusion and showed that the uptake efficiency of CP70Dc in homologous cells was increased after ECM addition. The uptake efficiency of ECM-293T-CP70Dc was only slightly increased, and those of CM-HepG2-CP70Dc and ECM-HeLa-CP70Dc were increased by approximately 10 and 20%, respectively, compared with that of CP70Dc (Figure 12c).

3.7.2. In Vitro Gene Transfection of ECM-CPDc. The analysis results of gene transfection efficiency for different ECM-CP70Dcs in vitro are shown in Figure 13. The EGFP expression efficiency of ECM-CP70Dc was increased compared with that of CDP70c, but the difference was not significant (Figure 13a). Similar to CP70Dc, the three ECM-CP70Dcs exhibited high EGFP expression in homologous cells but showed low gene transfection efficiency in HepG2 and HeLa cells. Flow cytometry results (Figure 13b) showed that compared with that of 293T-CP70Dc, the transfection efficiency of ECM-293T-CP70Dc was only slightly increased in homologous 293T cells (Figure 13c). The transfection efficiency of ECM-HepG2-CP70Dc was increased by nearly 20% in HepG2 cells but did not increase significantly in 293T and HeLa cells. Similarly, the transfection efficiency of ECM-HeLa-CP70Dc in HeLa cells was increased by 40%. These results suggested that the ECM could improve the homologous targeting of CPDcs but not their uptake and transfection efficiency in nonhomologous cells. Comparing the transfection efficiency of CPDc and ECM-CPDc in vitro, it could find that the transfection efficiency of ECM-CPDc in 293T cells was slightly higher than that of CPDc, which meant that ECM doping was beneficial to the transfection efficiency of CPDc, although not significant. ECM doping did not show an advantage in the transfection efficiency of CPDc in other cells, which might be because 293T cells were conducive to the uptake and transfection of foreign gene substances. Therefore, if we want to further promote the transfection efficiency by ECM doping, the ECM doped on ECM-CPDc may need to be accurately quantified.

4. NOVELTY STATEMENT

This work further investigated the application of the cell membrane as a safe material in gene delivery. Different cancer cell membranes were used to encapsulate PEI/DNA complexes to prepare safe and efficient gene delivery systems, which was named CPDc. Compared with the PEI/DNA complex, CPDc showed better safety and significant homologous targeting with the encapsulated cell membrane, especially the PEI/DNA complex encapsulated in the 293T cell membrane (293T-CPDc). Moreover, it also studied the effect of extracellular substances on CPDc as a gene delivery system. The results showed that the transfection efficiency and homologous targeting of CPDc were further improved by the doping of extracellular substances.

AUTHOR INFORMATION

Corresponding Author

Liang Liu − *College of Life Science and Technology, Wuhan Polytechnic University, Wuhan 430023, China;* orcid.org/0000-0002-3182-0541; Email: hustll@126.com

Authors

Yiran Chen − *College of Life Science and Technology, Wuhan Polytechnic University, Wuhan 430023, China*

Chaobing Liu − *College of Life Science and Technology, Wuhan Polytechnic University, Wuhan 430023, China*

Yujian Yan − *College of Life Science and Technology, Wuhan Polytechnic University, Wuhan 430023, China*

Zhaojun Yang − *College of Life Science and Technology, Wuhan Polytechnic University, Wuhan 430023, China*

Xin Chen − *College of Life Science and Technology, Wuhan Polytechnic University, Wuhan 430023, China*

Gang Liu − *School of Food Science and Engineering, Wuhan Polytechnic University, Wuhan 430023, China;* orcid.org/0000-0002-1610-6729

Complete contact information is available at: https://pubs.acs.org/10.1021/acs.molpharmaceut.1c00359

Notes

The authors declare no competing financial interest.

https://doi.org/10.1021/acs.molpharmaceut.1c00359
Mol. Pharmaceutics 2021, 18, 2803−2822

■ ACKNOWLEDGMENTS

This work was supported by the National Natural Science Foundation of China (21602166), the Natural Science Foundation of Hubei Province (2020CFB760), and the Research and Innovation Initiatives of WHPU (2021Y11).

■ REFERENCES

(1) Fernandez-Piñeiro, I.; Pensado, A.; Badiola, I.; Sanchez, A. Development and characterisation of chondroitin sulfate- and hyaluronic acid-incorporated sorbitan ester nanoparticles as gene delivery systems. *Eur. J. Pharm. Biopharm.* **2018**, *125*, 85−94.

(2) Nam, J. P.; Kim, S.; Kim, S. W. Design of PEI-conjugated bioreducible polymer for efficient gene delivery. *Int. J. Pharm.* **2018**, *545*, 295−305.

(3) Olden, B. R.; Cheng, Y.; Yu, J. L.; Pun, S. H. Cationic polymers for non-viral gene delivery to human T cells. *J. Controlled Release* **2018**, *282*, 140−147.

(4) Taranejoo, S.; Chandrasekaran, R.; Cheng, W.; Hourigan, K. Bioreducible PEI-functionalized glycol chitosan: A novel gene vector with reduced cytotoxicity and improved transfection efficiency. *Carbohydr. Polym.* **2016**, *153*, 160−168.

(5) Tsai, C. W.; Lin, Z. W.; Chang, W. F.; Chen, Y. F.; Hu, W. W. Development of an indolicidin-derived peptide by reducing membrane perturbation to decrease cytotoxicity and maintain gene delivery ability. *Colloids Surf., B* **2018**, *165*, 18−27.

(6) Jeong, G. W.; Nah, J. W. Evaluation of disulfide bond-conjugated LMWSC-g-bPEI as non-viral vector for low cytotoxicity and efficient gene delivery. *Carbohydr. Polym.* **2017**, *178*, 322−330.

(7) Jiang, H.; Wang, S.; Zhou, X.; Wang, L.; Ye, L.; Zhou, Z.; Tang, J.; Liu, X.; Teng, L.; Shen, Y. New path to treating pancreatic cancer: TRAIL gene delivery targeting the fibroblast-enriched tumor microenvironment. *J. Controlled Release* **2018**, *286*, 254−263.

(8) Joshi, C. R.; Raghavan, V.; Vijayaraghavalu, S.; Gao, Y.; Saraswathy, M.; Labhasetwar, V.; Ghorpade, A. Reaching for the Stars in the Brain: Polymer-Mediated Gene Delivery to Human Astrocytes. *Mol. Ther.–Nucleic Acids* **2018**, *12*, 645−657.

(9) Elfinger, M.; Maucksch, C.; Rudolph, C. Characterization of lactoferrin as a targeting ligand for nonviral gene delivery to airway epithelial cells. *Biomaterials* **2007**, *28*, 3448−3455.

(10) Farris, E.; Sanderfer, K.; Lampe, A.; Brown, D. M.; Ramer-Tait, A. E.; Pannier, A. K. Oral Non-Viral Gene Delivery for Applications in DNA Vaccination and Gene Therapy. *Curr. Opin. Biomed. Eng.* **2018**, *7*, 51−57.

(11) Dhanya, G. R.; Caroline, D. S.; Rekha, M. R.; Sreenivasan, K. Histidine and arginine conjugated starch-PEI and its corresponding gold nanoparticles for gene delivery. *Int. J. Biol. Macromol.* **2018**, *120*, 999−1008.

(12) Salmasi, Z.; Mokhtarzadeh, A.; Hashemi, M.; Ebrahimian, M.; Farzad, S. A.; Parhiz, H.; Ramezani, M. Effective and safe in vivo gene delivery based on polyglutamic acid complexes with heterocyclic amine modified-polyethylenimine. *Colloids Surf., B* **2018**, *172*, 790−796.

(13) Ita, K. Polyplexes for gene and nucleic acid delivery: Progress and bottlenecks. *Eur. J. Pharm. Sci.* **2020**, *150*, No. 105358.

(14) Liu, L.; Yan, Y.; Ni, D.; Wu, S.; Chen, Y.; Chen, X.; Xiong, X.; Liu, G. TAT-functionalized PEI-grafting rice bran polysaccharides for safe and efficient gene delivery. *Int. J. Biol. Macromol.* **2020**, *146*, 1076−1086.

(15) Memaria, E.; Maghsoudib, A.; Yazdianc, F.; Yousefid, M.; Mohammadi, M. Synthesis of PHB-co-PEI nanoparticles as gene carriers for miR-128-encoding plasmid delivery to U87 glioblastoma cells. *Colloids Surf., A* **2020**, *599*, No. 124898.

(16) Lv, P.; Zhou, C.; Zhao, Y.; Liao, X.; Yang, B. Modified - epsilon - polylysine - grafted - PEI - beta - cyclodextrin supramolecular carrier for gene delivery. *Carbohydr. Polym.* **2017**, *168*, 103−111.

(17) Zhang, Y.; Lin, L.; Liu, L.; Liu, F.; Maruyama, A.; Tian, H.; Chen, X. Ionic-crosslinked polysaccharide/PEI/DNA nanoparticles for stabilized gene delivery. *Carbohydr. Polym.* **2018**, *201*, 246−256.

(18) Park, J. S.; Yi, S. W.; Kim, H. J.; Park, K. H. Receptor-mediated gene delivery into human mesenchymal stem cells using hyaluronic acid-shielded polyethylenimine/pDNA nanogels. *Carbohydr. Polym.* **2016**, *136*, 791−802.

(19) Guan, X.; Guo, Z.; Lin, L.; Chen, J.; Tian, H.; Chen, X. Ultrasensitive pH Triggered Charge/Size Dual-Rebound Gene Delivery System. *Nano Lett.* **2016**, *16*, 6823−6831.

(20) Xie, Y.; Kim, N. H.; Nadithe, V.; Schalk, D.; Thakur, A.; Kilic, A.; Lum, L. G.; Bassett, D. J. P.; Merkel, O. M. Targeted delivery of siRNA to activated T cells via transferrin-polyethylenimine (Tf-PEI) as a potential therapy of asthma. *J. Controlled Release* **2016**, *229*, 120−129.

(21) Zhao, L.; Li, Y.; Pei, D.; Huang, Q.; Zhang, H.; Yang, Z.; Li, F.; Shi, T. Glycopolymers/PEI complexes as serum-tolerant vectors for enhanced gene delivery to hepatocytes. *Carbohydr. Polym.* **2019**, *205*, 167−175.

(22) Fang, R. H.; Hu, C. M.; Luk, B. T.; Gao, W.; Copp, J. A.; Tai, Y.; O'Connor, D. E.; Zhang, L. Cancer cell membrane-coated nanoparticles for anticancer vaccination and drug delivery. *Nano Lett.* **2014**, *14*, 2181−2188.

(23) Nie, D.; Dai, Z.; Li, J.; Yang, Y.; Xi, Z.; Wang, J.; Zhang, W.; Qian, K.; Guo, S.; Zhu, C.; Wang, R.; Li, Y.; Yu, M.; Zhang, X.; Shi, X.; Gan, Y. Cancer-Cell-Membrane-Coated Nanoparticles with a Yolk-Shell Structure Augment Cancer Chemotherapy. *Nano Lett.* **2020**, *20*, 936−946.

(24) Li, J.; Zhen, X.; Lyu, Y.; Jiang, Y.; Huang, J.; Pu, K. Cell membrane coated semiconducting polymer nanoparticles for enhanced multimodal cancer phototheranostics. *ACS Nano* **2018**, *12*, 8520−8530.

(25) Moss, K. H.; Popova, P.; Hadrup, S. R.; Astakhova, K.; Taskova, M. Lipid Nanoparticles for Delivery of Therapeutic RNA Oligonucleotides. *Mol. Pharmaceutics* **2019**, *16*, 2265−2277.

(26) Fang, R. H.; Hu, C. M.; Chen, K. N.; Luk, B. T.; Carpenter, C. W.; Gao, W.; Li, S.; Zhang, D. E.; Lu, W.; Zhang, L. Lipid-insertion enables targeting functionalization of erythrocyte membrane-cloaked nanoparticles. *Nanoscale* **2013**, *5*, 8884−8888.

(27) Ewe, A.; Panchal, O.; Pinnapireddy, S. R.; Bakowsky, U.; Przybylski, S.; Temme, A.; Aigner, A. Liposome-polyethylenimine complexes (DPPC-PEI lipopolyplexes) for therapeutic siRNA delivery in vivo. *Nanomedicine* **2017**, *13*, 209−218.

(28) Schäfer, J.; Hobel, S.; Bakowsky, U.; Aigner, A. Liposome-polyethylenimine complexes for enhanced DNA and siRNA delivery. *Biomaterials* **2010**, *31*, 6892−6900.

(29) Shah, H.; Tariq, I.; Engelhardt, K.; Bakowsky, U.; Pinnapireddy, S. R. Development and Characterization of Ultrasound Activated Lipopolyplexes for Enhanced Transfection by Low Frequency Ultrasound in In Vitro Tumor Model. *Macromol. Biosci.* **2020**, *20*, No. 2000173.

(30) Hu, Q.; Gu, Z. In *Cell Membrane-Mediated Anticancer Drug Delivery*, Nanotechnology: Delivering on the Promise, Volume 2 2016; pp 197−211.

(31) Luk, B. T.; Zhang, L. Cell membrane-camouflaged nanoparticles for drug delivery. *J. Controlled Release* **2015**, *220*, 600−607.

(32) Gao, C.; Lin, Z.; Wu, Z.; Lin, X.; He, Q. Stem-cell-membrane camouflaging on near-infrared photoactivated upconversion nanoarchitectures for in vivo remote-controlled photodynamic therapy. *ACS Appl. Mater. Interfaces* **2016**, *8*, 34252−34260.

(33) Sun, H.; Su, J.; Meng, Q.; Yin, Q.; Chen, L.; Gu, W.; Zhang, P.; Zhang, Z.; Yu, H.; Wang, S.; Li, Y. Cancer-cell-biomimetic nanoparticles for targeted therapy of homotypic tumors. *Adv. Mater.* **2016**, *28*, 9581−9588.

(34) Xu, L.; Anchordoquy, T. J. Effect of cholesterol nanodomains on the targeting of lipid-based gene delivery in cultured cells. *Mol. Pharmaceutics* **2010**, *7*, 1311−1317.

(35) Harris, J. C.; Scully, M. A.; Day, E. S. Cancer Cell Membrane-Coated Nanoparticles for Cancer Management. *Cancers* **2019**, *11*, No. 1836.

(36) Liu, C. M.; Chen, G. B.; Chen, H. H.; Zhang, J. B.; Li, H. Z.; Sheng, M. X.; Weng, W. B.; Guo, S. M. Cancer cell membrane-

https://doi.org/10.1021/acs.molpharmaceut.1c00359
Mol. Pharmaceutics 2021, 18, 2803−2822

cloaked mesoporous silica nanoparticles with a pH-sensitive gatekeeper for cancer treatment. *Colloids Surf., B* **2019**, *175*, 477−486.
(37) Rao, L.; Bu, L. L.; Meng, Q. F.; Cai, B.; Deng, W. W.; Li, A.; Li, K.; Guo, S. S.; Zhang, W. F.; Liu, W.; et al. Antitumor platelet-mimicking magnetic nanoparticles. *Adv. Funct. Mater.* **2017**, *27*, No. 1604774.
(38) Lama, M.; Fernandes, F. M.; Marcellan, A.; Peltzer, J.; Trouillas, M.; Banzet, S.; Grosbot, M.; Sanchez, C.; Giraud-Guille, M. M.; Lataillade, J. J.; Coulomb, B.; Boissiere, C.; Nassif, N. Self-Assembled Collagen Microparticles by Aerosol as a Versatile Platform for Injectable Anisotropic Materials. *Small* **2020**, *16*, No. 1902224.
(39) Lee, H. J.; Mun, S.; Pham, D. M.; Kim, P. Extracellular Matrix-Based Hydrogels to Tailoring Tumor Organoids *ACS Biomater. Sci. Eng.* 2021, DOI: 10.1021/acsbiomaterials.0c01801.
(40) Tomaszewski, C. E.; DiLillo, K. M.; Baker, B. M.; Arnold, K. B.; Shikanov, A. Sequestered cell-secreted extracellular matrix proteins improve murine folliculogenesis and oocyte maturation for fertility preservation *Acta Biomater.* 2021, DOI: 10.1016/j.actbio.2021.03.041.

https://doi.org/10.1021/acs.molpharmaceut.1c00359
Mol. Pharmaceutics 2021, 18, 2803−2822